Journal of Marine Research, 56, 257–291, 1998

Tidal resuspension and deposition of particulate matter in the Oyster Grounds, North Sea

by Wim Van Raaphorst[1], Hans Malschaert[1] and Hans Van Haren[1]

ABSTRACT

Moored current meters, fluorometers and transmissometers were used in combination with sediment traps (aspect ratio >4) and shipborne sampling to determine fluxes of deposition and resuspension of total suspended matter (TSM) under tidal action in the 45 m deep Oyster Grounds, North Sea. Here, we present data from the mixed layer below the major thermocline at about 20 m above the bottom (mab) as obtained during a 14-day period of calm weather in July 1994. Around neap tide near-bottom current velocities remained smaller than 0.15 m s^{-1} and TSM was dominated by particles advected from a relatively turbid area to the southeast of the study site. At the onset of spring tide, current speeds increased with maximum values greater than 0.20 m s^{-1} and seabed friction velocities exceeding the threshold value for resuspension. Particles resuspended were strongly enriched with organic carbon compared to the bulk sediment, suggesting that not the bed proper but a fine-grained fluff fraction was eroded. This resuspended fluff was by far the dominant source for the mass fluxes in the sediment trap (at 3.2 mab), which showed a distinct tidal cycle with highest fluxes directly after low water slack tide and lowest fluxes during maximum ebb current. This pattern was caused by variations in apparent settling velocity of TSM, presumably due to floc formation during periods in the tidal cycle when current speeds were low and relatively high concentrations of both chlorophyll-*a* and TSM were found. From a simple model on advection, deposition and resuspension of TSM, we calculated a net accumulation on the sediment of 75 g m^{-2} during the 14-day study period, which is the difference between gross fluxes of deposition and resuspension. Upon deposition, the average retention time of particles until their next resuspension is calculated at 1–2 weeks, which may be sufficient for substantial decomposition of organic matter associated with TSM. This implies that, upon resuspension, particles transported further along the shelf are relatively poor in organic carbon. It is concluded that the Oyster Grounds serve as a mid-shelf temporary depocenter and that mineralization in this and similar areas may play a crucial role in the carbon budget of the North Sea.

1. Introduction

Deposition and resuspension of organic carbon and other elements associated with total suspended matter (TSM) form the major link between processes in the water column and the underlying sediment. In shallow shelf seas the time necessary for vertical transport from the productive surface layer of the water column to the seafloor is relatively short, and a considerable portion of primary production may reach the bottom (Jørgensen, 1983). For

1. Netherlands Institute for Sea Research (NIOZ), P.O. Box 59, 1790 AB Den Burg, The Netherlands.

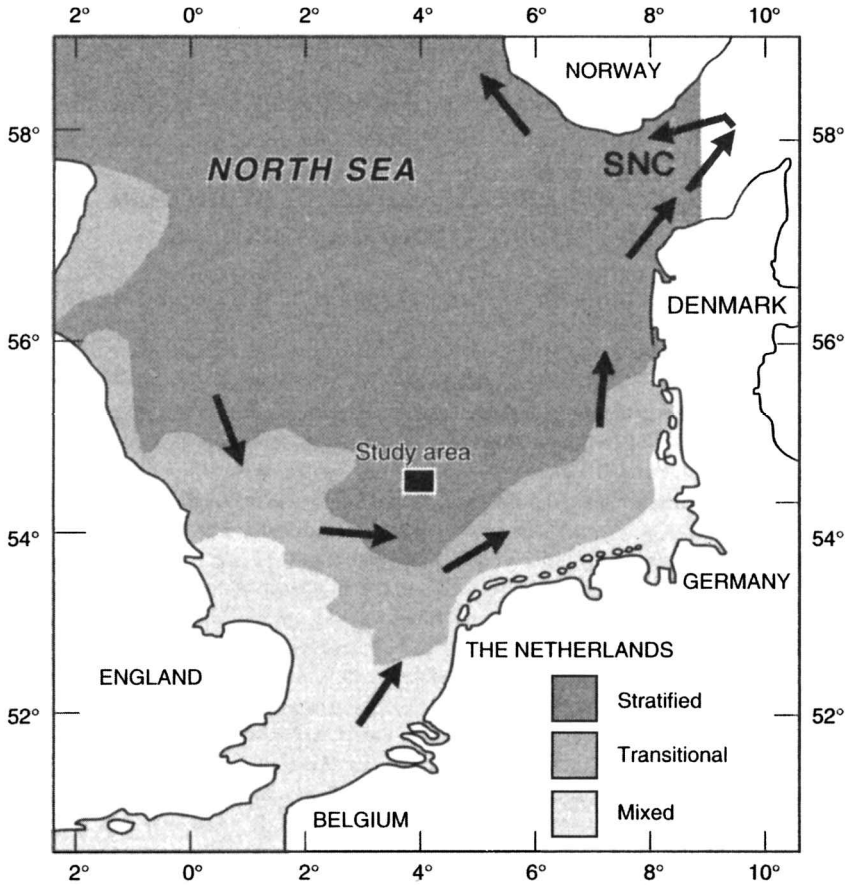

Figure 1. Map of the North Sea, the box showing the position of the study site in the Oyster Grounds. The shading indicates whether the water column is well mixed or stratified in summer. These areas correspond to the bathymetry: mixed <30 m deep, transitional 30–40 m deep, stratified 40–200 m deep. In the Skagerrak/Norwegian Channel (SNC) the water depth is >200 m. Arrows indicate the large-scale transport route of water and TSM in the North Sea.

the North Sea it has been estimated that 17–45% of the primarily produced organic C is mineralized in the sediments (Postma and Rommets, 1984; Nedwell *et al.,* 1993). Shelf seas are, however, highly energetic and a portion of detrital particles may be kept in suspension or may be resuspended from the bottom by wave action and tidal currents (Jago *et al.,* 1993; Churchill *et al.,* 1994). As a consequence, a considerable amount of particulate organic matter may be swept from the shelf to the depocenters on the continental slope where it is further mineralized or buried in the sedimentary record (Walsh, 1991). In the North Sea the main depocenter is found in the Skagerrak/Norwegian Channel (SNC, Fig. 1) where about 50–70% of the total mass accumulation occurs (Eisma and Kalf, 1987).

The average time scale for water transport from the southern and central North Sea to the

SNC is several months to, essentially, less than one year (Hainbucher *et al.,* 1987; Otto *et al.,* 1990). Since 'fresh' marine phytoplankton debris typically has first order decomposition rates in the order of 10 y^{-1} (Walsh *et al.,* 1988; Middelburg, 1989; Van Raaphorst *et al.,* 1992) such a transport time would be sufficient to enable almost complete loss of organic matter; about 99% of the organic matter would be mineralized during six months of transport. Even when taking into account that the decomposition rate decreases as the substrate ages (Middelburg, 1989), most of the original organic matter would be mineralized during transport across the North Sea. Using the power-model of Middelburg (1989) with an initial 'age' of the organic matter of 10^{-4} y and a power of 0.16, only about 10% would remain after six months. This supports earlier conclusions that, apart from local production (Kempe and Jennerjahn, 1988), the organic matter finally deposited in the SNC is largely of refractory nature (Van Weering *et al.,* 1987; Kempe *et al.,* 1988; Lohse *et al.,* 1995).

Particulate matter passes through many cycles of settling and resuspension during transport over the shelf (Eisma and Kalf, 1987; Van Weering *et al.,* 1987; Kempe *et al.,* 1988). Depending on the hydrodynamic conditions, particles are stored over a range of time scales in what may be called temporary depocenters on the shelf. Puls and Sündermann (1990) and Sündermann (1993) demonstrated that particles derived from the East Anglian turbidity plume and the southern North Sea can settle in the Oyster Grounds in spring and summer, although net annual accumulation probably is of minor importance in that area (Cadée, 1984; Eisma and Kalf, 1987). By considering tidal currents only, Creutzberg and Postma (1979) concluded that it should be possible for fine particles to settle in the Oyster Grounds. The absence of net accumulation then suggests that such settlement can only be temporary and that particles are eroded again during, e.g., autumn and winter storms (Kempe *et al.,* 1988, Puls and Sündermann, 1990).

Transient deposition contains relatively fresh plankton debris that may serve as food for the local benthic fauna (Jenness and Duineveld, 1985). Upon settlement, organic C is mineralized and nutrients are largely recycled from the pore waters to the water column (Nedwell *et al.,* 1993; Gehlen *et al.,* 1995; Lohse *et al.,* 1995) thus stimulating primary production in the area of temporary deposition. On the other hand, upon resuspension, turbidity of the water increases, thus putting limits to the local primary production (Tett and Walne, 1995). Rather than the permanent depocenters on the continental slope which are being fueled by aged materials, the temporary depocenters on the shelf represent key areas for the benthic turnover of organic matter in the North Sea (Gehlen *et al.,* 1995; Lohse *et al.,* 1995).

Deposition and resuspension of TSM in the temporary depocenters have to be considered to understand the carbon budget of shelf seas. Field studies on this subject mostly focus on sediment movement during periods of erosion (Moody *et al.,* 1987; Churchill *et al.,* 1988, 1994; Drake and Cacchione, 1989; Lyne *et al.,* 1990a,b). Less attention seems to be paid to the tidal dynamics of TSM during fair weather conditions when settlement may prevail (e.g. Jago *et al.,* 1993). Here we present such data collected during the integrated

North Sea Mooring Programme (INP-Mooring) at a station in the Oyster Grounds in July 1994. For this study a sediment trap was deployed which sampled at a high rate (hourly) to resolve the tidal signal, and observations were made with moored sensors on transmission, fluorescence and currents. A simple model describing advection, deposition and resuspension of TSM was constructed to guide the discussion of the experimental data. The aim of our study was (1) to determine deposition and resuspension of TSM under tidal action and (2) to evaluate the implications for transport and temporary deposition of TSM in the North Sea.

2. Materials and methods

a. Study site

The measurements were performed during a cruise with the RV *Pelagia* in a small grid (about 1×1 km) between 54°24′9″–54°25′5″N and 4°01′9″–4°02′9″E in the Oyster Grounds on the transition between the southern and the central North Sea (Fig. 1). Water depth at the site is 45.5 ± 0.5 m, with the major thermocline around 25–27 m depth. The tidal range is about 1 m at mean spring tide. Data were collected between 5 and 19 July 1994 (day numbers 185 and 199, respectively). On 7 and 8 July 1994 an additional survey was made covering 55 CTD stations in a larger area between 54°15′–54°35′N and 3°45′–4°19′E.

The experimental site is in the area where Sündermann (1993) predicted deposition of TSM. Tidal mixing fronts frequently occur about 90 km south of the mooring grid where water masses from the southern and northern/central North Sea meet (Pingree and Griffiths, 1978; Van Haren and Joordens, 1990). According to the Wenthworth scale of the bottom, sediment consists of very fine sand with a median grain size of $\sim$100 μm (Lohse *et al.,* 1995), a fraction $\sim$15% $<$ 63 μm and a fraction $\sim$5% $<$ 6 μm (Van Raaphorst and Malschaert, 1996). Most of the fine particles present have been identified as 'relicts' from Holocene origin (Cadée, 1984; Eisma and Kalf, 1987). TSM in the bottom water consists of the constituent particles with a mean diameter of 5–10 μm aggregating to flocs of 100–300 μm, depending on the season and weather conditions (Chen, 1995). POC content of TSM is normally between 10 and 20% below the thermocline during summer (Postma and Rommets, 1984; Hölemann and Wirth, 1988).

b. Field techniques

Wind velocity and direction were obtained from platform F3 $\sim$60 km NE, wave data from platform K13 $\sim$200 km SW of the mooring grid. Water samples were collected with 25-liter Niskin bottles at 6, 11, 21, 31 and 41 m above the bottom (mab) 14 times spread over the study period and at different phases of the tidal cycle. Additional samples were drawn from 0.2 mab using a membrane pump. The first 200 l pumped on deck were discarded before filling carboys of 25-liter. The rate of pumping was 12–18 l min^{-1} resulting in vertical flow velocities through the tubing >1 m s^{-1}. All materials were made

of polypropylene or polythene and cleaned before use. The carboys were carefully homogenized and TSM was collected by low-pressure filtration of 0.5 l subsamples over pre-weighed 0.4 μm polycarbonate filters (25 mm diameter) and subsequently rinsing the filters with milliQ water to remove the salt. Additional volumes of 0.5 l were filtered (25 mm GF/F, pre-heated at 400°C) for analyzing POC and PON in TSM.

Usually, CTD casts were performed once or twice a day, and at 1 h intervals during a full tidal cycle on 5 and 6 July 1994. The Seabird 911 CTD was equipped with a Sea-Tech transmissometer (660–670 nm, 0.25 m light path). The light attenuation coefficient was calculated from c_0 = ln(transmission)/light path and calibrated against TSM measured by filtration. All transmission data are expressed as TSM in mg l^{-1}. The fluorometer mounted on the CTD was a Chelsea Instruments Aquatracka with a excitation wavelength of 440 nm and band width of 80 nm, and a detection wavelength of 670 nm and band width of 30 nm. All fluorescence data were converted to units of chlorophyll-*a* using the *in situ* concentrations of chlorophyll-*a* measured on HPLC by Van Duyl *et al.* (1997) for calibration.

An extensive set of moored sensors was deployed at the site. Here we present data based on 10 min. ensembles from the current meter (NBA-DNC 2M) placed at 1.5 mab. Accuracy of the current data is ±1 cm s^{-1} and ±5° TN for speed and direction, respectively. We have no data from 'normal' transmissometers moored below the thermocline during the study period. Instead, the light attenuation coefficient was obtained from the 'transmission blank' measured by the WS Oceans NAS-1 submersible nitrate analyser, sampling at 1-h intervals at a 560 nm, and a 0.02 m light path, moored at 4.5 mab. The attenuation data from the NAS-1 were calibrated against those obtained with the Sea-Tech transmissometer on the CTD. A Chelsea instruments Aquatracka MK-III fluorometer was moored at 5 mab. Filters used were selected to measure chlorophyll-*a* and had a bandwidth of 100 nm around a wavelength of 430 nm for excitation and a bandwidth of 30 nm around 685 nm for emission.

A Technicap PPS4/3 sediment trap (unbaffled, height 1.2 m, collecting area 0.05 m^2) was moored to collect TSM at 3.2 mab. A tilt meter was mounted on the mooring chain just below the trap. The trap has a cylindrical upper part of 0.55 m length and a 0.45 m excentric conical part (maximum angle 30°) below, ending in a funnel to the carousel with 12 sample cups (250 ml). Aspect ratio of the trap is 2.2 based on the cylindrical part only, and greater than 4 taking into account the full length. The trap was programmed daily to collect during 1-h intervals for a total period of 12 h, opening the first cup at 17.00 h UTC and closing the last cup at 5.00 h UTC the next day. Recovery of the trap was between 8 and 10 h local time. The cups were filled with filtered seawater (0.4 μm polycarbonate) from the study area before deployment, without addition of preservatives. Immediately after retrieval on deck the sample cups were transferred to a climate room at *in situ* bottom water temperature (9–10°C) for subsequent filtration over 200 μm plankton gauze and pre-weighed 0.45 μm HAc filters (45 mm diameter). The filters were stored at −20°C for further processing in the laboratory.

Sediment samples were obtained by gently pushing acrylic liners into the sediment

which was retrieved on deck by a cylindrical boxcorer (for details see Van Raaphorst and Malschaert, 1996). The boxcores were taken at distances of about 180 m from each other along the eastern and northern boundaries of the mooring grid, i.e. not between the moorings. The subcores were sliced in 2.5 to 20 mm thick layers at *in situ* temperature, and stored at −20°C. Here, only data from the upper two layers (0–2.5 mm and 2.5–5 mm) will be discussed.

c. *Laboratory analysis*

Water content of the sediment samples was obtained from the loss of weight after drying at 60° for 48 h. Filters containing TSM and trap material were dried (60°C, 24 h) and re-weighed for mass calculation. POC and PON content of sediment samples and trap material, scraped carefully from the filters (under binoculars, harvest ∼95%), was determined on a Carlo Erba NA 1500-2 elemental analyzer following the procedure of Verardo *et al.* (1990). Inorganic C was removed from the samples by addition of sulphurous acid. For the POC and PON contents of TSM, the complete GF/F filters were used. Accuracy expressed as the coefficient of variation for replicate samples was ∼2.5% for POC, ∼7% for PON and ∼4% for the CN ratio.

d. *The model*

The concentration of particles in the water column is determined by advection, deposition, resuspension, vertical mixing and internal sources and sinks:

$$\frac{\partial C}{\partial t} + \frac{\partial (uC)}{\partial x} + \frac{\partial (vC)}{\partial y} - \frac{\partial (\omega C)}{\partial z} = \frac{\partial}{\partial z}\left(K\frac{\partial C}{\partial z}\right) + S \qquad (1)$$

where C is the mass concentration (g m^{-3}), t is time (s), u, v are fluid velocities (m s^{-1}) in the x (east-west) and y direction (north-south), respectively, ω is the settling velocity of suspended particles (m s^{-1}), K is the vertical eddy diffusivity (m^2 s^{-1}) and S is a combined source/sink term (g m^{-3} s^{-1}). Vertical fluid velocity and horizontal dispersion are neglected in this equation and all parameters may, in principle, be variable in time and x, y, z direction. The term S includes phytoplankton production of POC but also, for a given size class of particles, losses to and gains from other size classes through flocculation and de-flocculation (Hill and Nowell, 1995). If, as a first approximation, it is assumed that the dynamics of suspended particles can be described in terms of quantities averaged over all size classes, and if it is further assumed that net production of POC is small on the time-scales considered, (1) is valid for TSM with $S = 0$.

The next simplification is made by assuming that the velocities u and v are essentially constant on the length scales of the mooring grid so that the advection terms in (1) may be replaced by the products of u, v and the horizontal concentration gradients. After taking the

average of (1) over the bottom mixed layer, this yields the model applied in this study:

$$\frac{\partial \langle C \rangle}{\partial t} + \left\langle u\frac{\partial C}{\partial x}\right\rangle + \left\langle v\frac{\partial C}{\partial y}\right\rangle = \frac{1}{h}\left(K_b\left\langle\frac{\partial C}{\partial z}\right\rangle_b - (\omega C)_b\right) + \frac{1}{h}\left((\omega C)_h - K_h\left\langle\frac{\partial C}{\partial z}\right\rangle_h\right) \tag{2}$$

where $\langle\ \rangle$ is the layer average, h is the depth of the bottom mixed layer (in meters) and the subscripts h and b point at the upper (thermocline) and lower boundary (bottom), respectively.

At the bottom the boundary condition reads:

$$Kb\left\langle\frac{\partial C}{\partial z}\right\rangle_b - (\omega C)_b = E_b - Q_b \tag{3}$$

where Q_b is the rate of deposition on the bottom (g m^{-2} s^{-1}) and E_b is the resuspension flux (g m^{-2} s^{-1}). A similar condition may be formulated for the upper boundary. In our model, however, we assume that the vertical fluxes across the thermocline can be neglected. This assumption is justified from the consideration that in the study area by far the largest portion of TSM in the bottom mixed layer originates from the sediment or is advected in suspension (Jago *et al.,* 1993). Further support follows from the data of Van Duyl *et al.* (1997) which show that only minor quantities of phytoplankton pigments settled from the surface layer to the bottom layer during the period of study. Thus, the last term in brackets on the right-hand side of (2) is set to zero.

Application of the model is intended to demonstrate the influence of advection, deposition and resuspension on the particle concentrations in the bottom mixed layer. Following the results of Jago *et al.* (1993) a constant background concentration C_{back} of TSM is assumed in the model, consisting of particles with such a small settling velocity that they are uniformly distributed over depth and do not settle on the seafloor. This background concentration is one of the fitting parameters of the model. The model details outlined below refer to TSM corrected for the background concentration.

i. Advection. The u and v velocities are taken from the current data at 1.5 mab, and the gradients $\partial C/dx$ and $\partial C/dy$ are based on transmission data from 6 mab obtained during the survey around the mooring grid on 7 and 8 July. We are aware that combining the data from these single depths may not be fully representative for the bottom mixed layer averaged advection of TSM, but nevertheless we believe that, given all other assumptions, this approximation is sufficiently accurate for our purpose.

ii. Deposition. The settling flux is assumed to be proportional to the TSM concentration C_b at the seafloor

$$Q_b = \omega C_b. \tag{4}$$

To estimate the concentration C_b at $z = 0$ downward settling fluxes and upward diffusive transport in the water column are assumed to balance:

$$C_z = \langle C \rangle \frac{h\omega}{K} \frac{\exp\left(\frac{-\omega}{K} z\right)}{1 - \exp\left(\frac{-\omega}{K} h\right)}. \tag{5}$$

In Eq. (5) the vertically constant eddy diffusivity K is related to the friction velocity U^*: $K = 0.16 \cdot U^*$ (Puls and Sündermann, 1993), where U^* (m s^{-1}) is calculated as $U^* = [C_D \times (u^2 + v^2)]^{0.5}$ and the drag coefficient $C_D = 2.5 \times 10^{-3}$. The concentration C_b at the bottom follows after inserting $z = 0$ in Eq. (5).

Eq. (5) yields similar profiles as the inverse power relation in the logarithmic bottom layer (e.g., Drake and Cacchione, 1989; Wright, 1995) but it has the advantage that it predicts finite concentrations at $z = 0$. For the settling velocity ω, a value of 2×10^{-5} m s^{-1} is chosen as an average for suspended fine particles in this part of the North Sea (Jago *et al.,* 1993; Pohlman and Puls, 1995; Tett and Walne, 1995). Applying Stokes law this settling velocity corresponds to a spherical particle diameter of ~6 μm, in accordance with the size of the nonflocculated particles observed by Chen (1995) in the Oyster Grounds. The dependency of C_b on K and U^* implies that deposition is most effective at slack tides when the current velocity is lowest. The above equation neglects the effect of the bed shear stress which reduces the portion of particles effectively settling on the seafloor (threshold for deposition cf. Krone, 1962). We tested the model with a formulation for such a threshold velocity for deposition included, but this did not improve the performance of the model. It is, therefore, assumed that the shear stress prevailing during the experiments is essentially low enough to facilitate complete deposition.

iii. Resuspension. The formulation for resuspension includes a threshold friction velocity below which no entrainment of particles from the seafloor can occur

$$E_b = \beta_r \cdot M_r \cdot \left(\frac{U_*^2}{U_{*,r}} - 1\right) \qquad \text{for } U_* \geq U_{*,r} \tag{6a}$$

and

$$E_b = 0 \qquad \text{for } U_* < U_{*,r} \tag{6b}$$

where β_r (s^{-1}) is the entrainment rate constant, M_r(g m^{-2}) is the total mass of particles on the seabed available for resuspension and $U_{*,r}$ is the threshold friction velocity. Values for this threshold vary considerably between sediment types and depend on several environmental factors (e.g., water content, bed form, biological activity). Here a value of 8×10^{-3} m s^{-1} is chosen, slightly below the value applied by Tett and Walne (1993) but much

lower than the threshold velocity applied by Puls and Sündermann (1993) and in several other erosion studies (e.g., Moody *et al.,* 1987; Drake and Cacchione, 1989; Churchill *et al.,* 1994). We assume, however, that only a loose layer of freshly settled fluff material is resuspended by tidal currents in the Oyster Grounds, and not material from the underlying bed (Jago *et al.,* 1993). Consequently, M_r is the mass of particles present in this fluff layer, calculated at each time step from the cumulative difference between deposition and resuspension during the previous period.

In the model resuspension causes a temporary increase in the average settling velocity of TSM lasting for 30 min after the resuspension event. Thereafter, ω returns to the basic 2×10^{-5} m s^{-1} until the next event. This increase is included to take into account the larger average floc size of the particles from the fluff layer. The increased settling velocity finally applied is estimated by visually fitting the model results to the experimental data.

The erosion rate β_r is not easily quantified from the literature, particularly not for the fluff particles involved here (Jago *et al.,* 1993). Therefore, this parameter has also been quantified from fitting the model to the field data.

3. Results

At the site, the ebb current runs in a westerly direction and the flood current to the east. Accordingly we will refer to the slack tide when the current turns from west to east as low water slack (LW), and when it turns from east to west as high water slack (HW).

a. Sediment

Visual inspection of the sediment cores showed brown-greenish fine sand in the upper centimeters with a thin darker brown fluffy layer on top, particularly in surface depressions, burrows and excavation mounds of the benthic fauna (mainly *Amphiura filiformis, Chaetopterus variopedatus* and *Calianassa subterranea*). This fluffy layer was most pronounced during the first few days of the study and almost disappeared later on.

The water content was about 0.02 g g^{-1} higher in the upper 2.5 mm than in the 2.5–5 mm depth interval (Fig. 2a). There was a tendency of decreasing water content after maximum values observed at days 187–189. The POC content of the sediment showed the same tendency in time with slightly, but consistently higher values around a mean content of 0.24% (SD = 0.04, n = 13) in the upper 2.5 mm compared to a mean value of 0.22% (SD = 0.04, n = 13) in the 2.5 mm below (Fig. 2b). The average CN ratio of the sediment was 10.8 (SD = 0.8, n = 13) in both depth intervals, without any visible trend in time (Fig. 2c).

b. Spatial distribution of chlorophyll-a and TSM

The survey around the mooring grid revealed an approximately east-west directed gradient in chlorophyll-*a* at 6 mab with the highest values west from the grid (Fig. 3a). Above the thermocline the spatial distribution of chlorophyll-a was more patchy without a

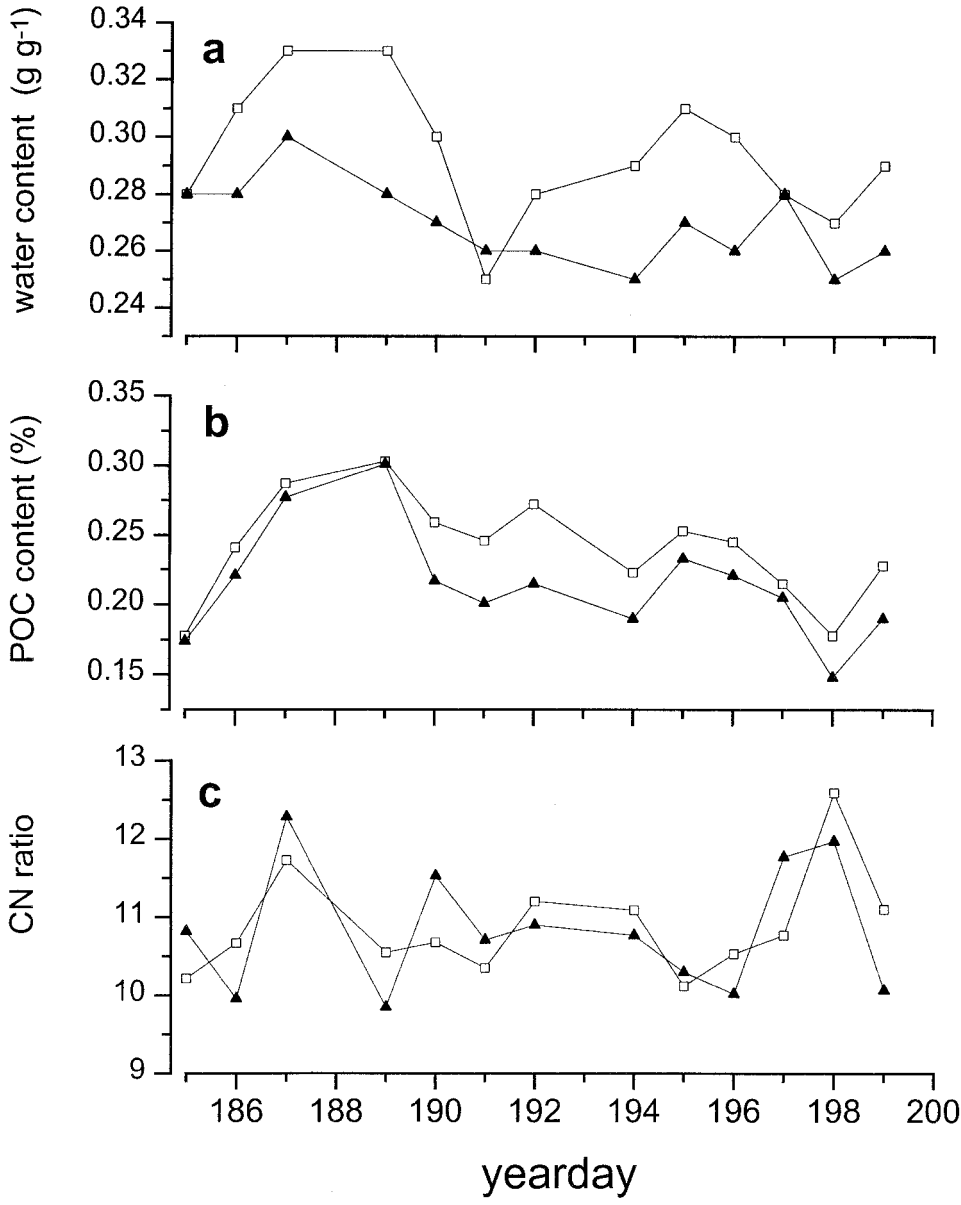

Figure 2. Properties of the upper sediment layers (0–2.5 mm open symbols, 2.5–5 mm filled symbols) at the mooring site between 5 and 19 July 1994 (days 185–199). a: water content; b: POC content of the solid particles; c: atomic CN ratio of the sedimentary organic matter.

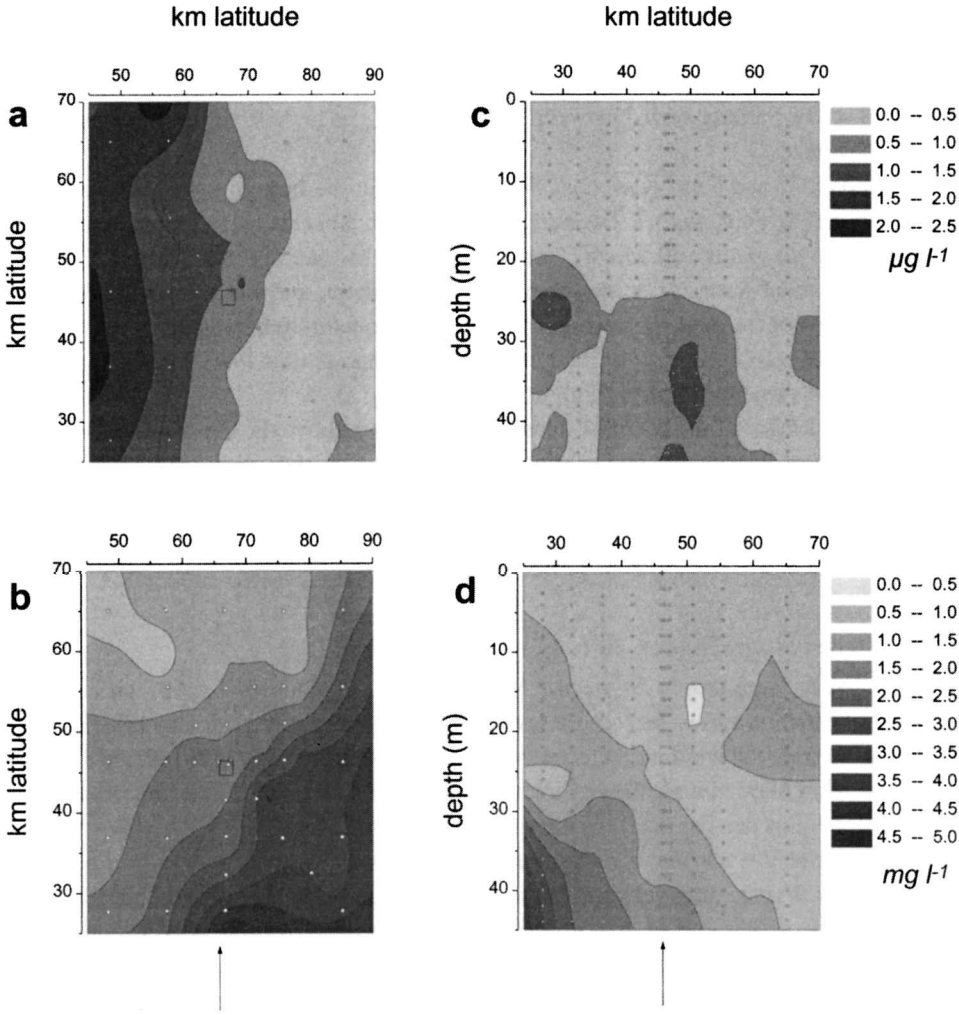

Figure 3. Spatial distribution of chlorophyll-*a* and TSM around the mooring grid on 7 and 8 July 1994. Panels a and b show the horizontal distributions of TSM and chlorophyll-*a*, respectively, at 6 mab, while panels c and d show their vertical distributions along the north-south section. The position of this section is marked with the arrow below (b). Dots indicate sampling points, boxes in (a,b) and arrow below (d) the position of the mooring grid.

clear gradient. In the bottom layer the TSM concentration showed a gradient with decreasing values from south-east to north-west (Fig. 3b,d). A similar distribution, though at lower concentrations, was present above the thermocline.

c. Vertical distribution of chlorophyll-a and TSM

The water column was stratified with a series of temperature transitions between 10 and 25 m depth on top of the major thermocline at 25–27 m depth (19–21 mab). Temperature

increased from 15°C at day 185 to 18°C at day 199 in the upper 10 m of the water column and from 9.2 to 9.8°C at 1.5 mab. Semi-diurnal variation of temperature was apparent, although small when compared to the gradual increase of the mean temperature during the period of study. Salinity varied between 34.3 and 34.7, the highest values occurring at the end of the cruise.

Chlorophyll-*a* and TSM were considerably higher in the bottom layer than above the thermocline (Fig. 3c,d, 4a,b). TSM increased with depth and reached maximum concentrations close to the bottom (0.2 mab) where concentrations were between 5 and 12 mg l^{-1} around LW, about 5 mg l^{-1} around maximum ebb current, and between 1 and 3 mg l^{-1} during the rest of the tidal cycle (Fig. 5). One exceptionally high value of 20 mg l^{-1} was measured just before maximum flood current at 0.2 mab at day 198. At all other depths TSM was less variable around 1–2 mg l^{-1} (Table 1, Fig. 5).

The POC content of the suspended matter was highest above the thermocline (Table 1). The CN ratio of the organic matter showed much less variation with depth and was also rather constant during the tidal cycle at values close to 10.5 (Table 1). At 21 mab the CN ratio appeared to be slightly lower, but the difference with the other depths is statistically not significant at $p = 0.1$ (Student's *t*-test, $n = 11$).

d. Time series of wind, current velocity, chlorophyll-a and TSM

Wind speeds were mostly between 2.5 and 7.5 m s^{-1}. Velocities higher than 7.5 m s^{-1} occurred, however, during periods of several hours between days 190 and 193 (Fig. 6a). During most days the wind was directed to the north, except at days 188–189 and 197–199 when the wind blew in a southerly direction. Wave action was of minor importance with significant heights smaller than 1 m throughout the period of study.

Current velocities showed a semi-diurnal tidal periodicity superimposed on a spring-neap cycle, with maximum velocities greater than 0.20 m s^{-1} at 1.5 mab around spring tide (day 192) and smaller than 0.15 m s^{-1} around neap tide (day 185 and 199). The main axis of the tidal ellipse was oriented approximately in the east-west direction, ~90° TN for the flood current and ~300° TN for the ebb current. The current (Fig. 6b) caused only a minor net east-west displacement over the 14 days experimental period (Fig. 6c). In accordance with the lateral gradient in chlorophyll-*a* (Fig. 3a), the east-west tidal current was responsible for advecting chlorophyll-*a* to the mooring site. From day 186 to 196 peaks in chlorophyll-*a* coincided with maximum displacement to the east around HW (Figs. 4a, 6f). After day 196 chlorophyll-*a* had a major peak around midnight with only a minor peak during the day, suggesting that the influence of a front with higher chlorophyll-*a* concentrations had ceased by that day. The moving average of the chlorophyll-*a* time series showed an increasing trend until day 189, followed by a gradual decrease (Fig. 6f).

The north-south component of the current was smaller and less regular than its east-west counterpart (Fig. 6d). Superimposed on the tidal sinusoidal form, the north-south current showed an additional minimum velocity at HW when the east-west current was about zero (Fig. 8a,b). Net tidal displacement, calculated from the time integral of the *u* and *v* current

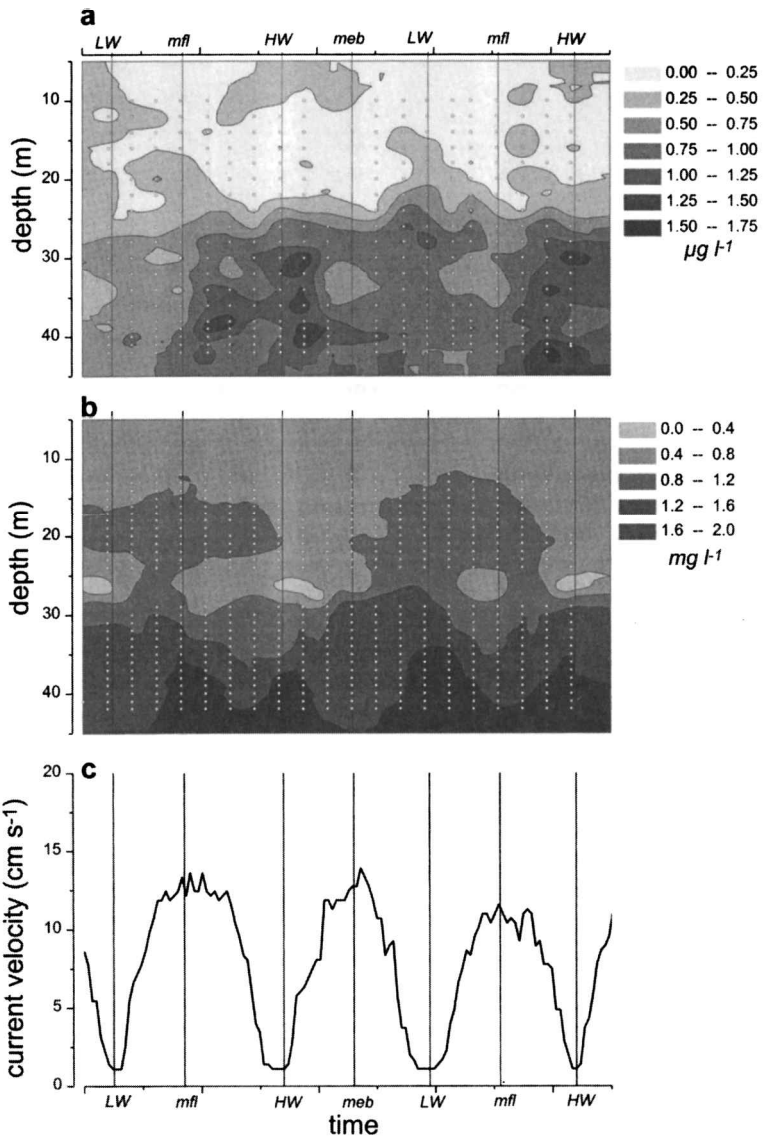

Figure 4. Vertical distribution of chlorophyll-*a* and TSM and the current velocity (1.5 mab) at the mooring site during a 24 h period on 7 and 8 July 1994. Dots indicate sampling points. HW = high water slack, LW = low water slack, mfl = maximum flood current, meb = maximum ebb current. (a) chlorophyll-*a*; (b) TSM, (c) current velocity.

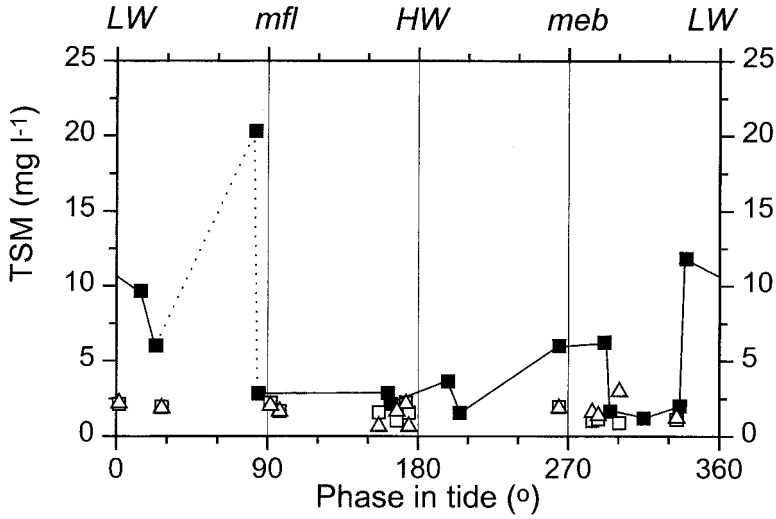

Figure 5. TSM in water samples obtained from 0.2 (■), 6 (△) and 11 (□) mab at different phases of the tidal cycle. Samples from several days were positioned in a mean tidal cycle relative to the moment of LW to convert the time of sampling into degrees with LW = 0°, 360° and HW = 180°; mfl = maximum flood current, meb = maximum ebb current. Data from 0.2 mab are joined for clarity. The exceptionally high value before mfl is suspect.

velocities, was much larger to the north than to the west (Fig. 6e). Time series of TSM showed moderate peaks (Fig. 6g). From the moving average of TSM we observed a slightly increasing trend until day 188 followed by a minimum at day 189. A more pronounced decrease occurred from day 197 to 198 corresponding with the few days when the wind blew to the south, a decreased rate of net tidal displacement to the north and a low maximum current speeds at neap tide (Fig. 6e).

e. Sediment traps

The tilt meter recordings indicated considerable inclinations of the trap, although always less than 25° from the vertical. The highest tilts were measured at maximum current

Table 1. Average concentration (and SD) of TSM, POC content and CN ratio measured in the bottle samples from different depths in the water column. The data from 0.2 mab represent bottom water sampled with a membrane pump, from 6–11 mab represents the lower water column, 21 mab is at the lower part of the thermocline, and 31–41 mab is in the surface mixed waters. The number of data varies from $n = 11$ (POC, 21 mab) to $n = 24$ (TSM, 6–11 and 31– 41 mab).

Depth mab	TSM mg l^{-1}	POC %	CN ratio
0.2	4.1 (3.4)	9.4 (5.1)	10.6 (2.9)
6–11	1.7 (0.6)	11.0 (5.8)	10.0 (3.0)
21	1.4 (0.7)	16.6 (8.5)	8.8 (1.9)
31–41	0.9 (0.5)	18.8 (8.5)	10.8 (4.5)

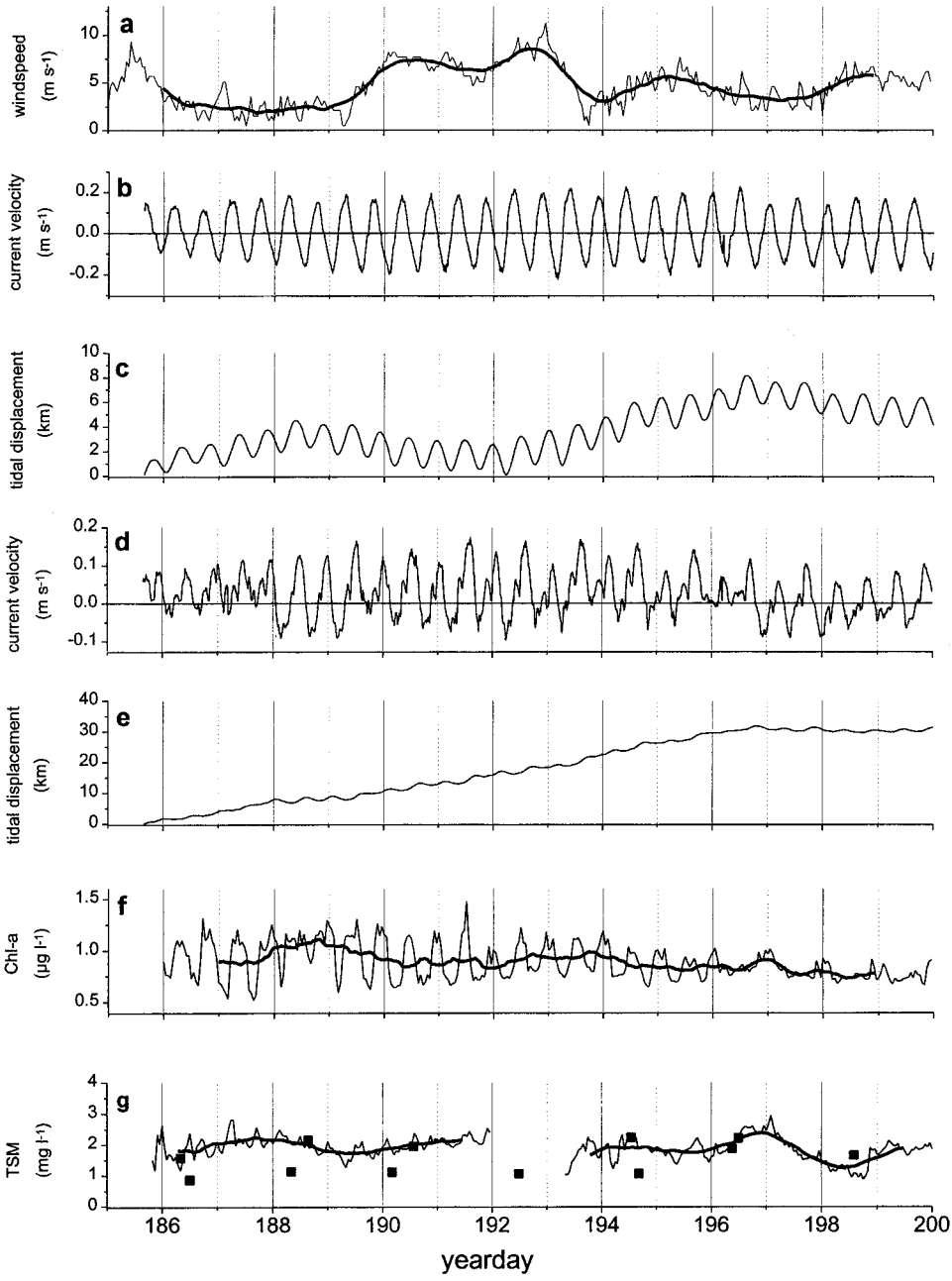

Figure 6. Time series of (a) wind speed at 10 m above the water surface, (b) current velocity in east-west direction at 1.5 mab, (c) net tidal displacement in east-west direction at 1.5 mab, (d) current velocity in north-south direction at 1.5 mab, (e) net tidal displacement in north-south direction at 1.5 mab, (f) chlorophyll-*a* at 5 mab, and (g) TSM at 4.5 mab. Thick lines are 12 h moving averages of the data. Currents to the north and to the east are positive. Thin line in (g) represents transmission data, ■ bottle data.

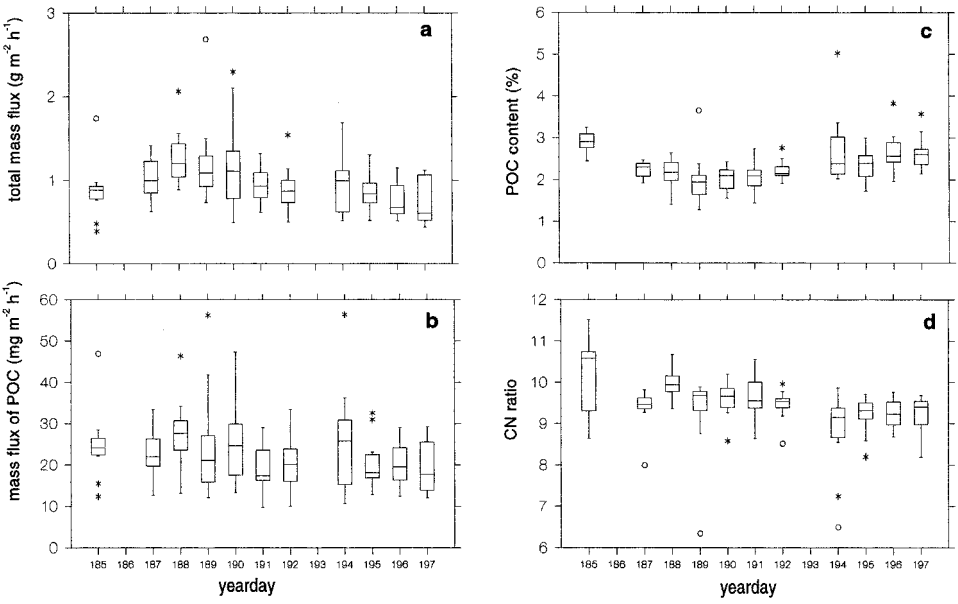

Figure 7. Time series of the tidally averaged mass fluxes in the sediment trap at 3.2 mab. In the box-whisker plots the horizontal line is the median value, the lower and upper side of the boxes are the 25th and 75th percentiles, respectively and the whiskers extend to the 5th and 95th percentiles, respectively. Exceptionally high and low individual data are indicated with an asterisk or an open circle, depending on the distance from the median value (approximately 2 and 3.5 times the box size, respectively). (a) Total mass flux of dry weight; (b) mass flux of POC; (c) POC content of particles trapped; (d) atomic CN ratio of the trapped organic matter.

velocities. Here we give the trap results uncorrected for tilt, and we will come back to this point in the discussion.

Inspection under the microscope showed that the material caught in the trap consisted mainly of fine grained sediment particles (silt). Diatoms or their remains were visible and one or two copepods had entered some of the sample cups. Total mass fluxes (dry weight) were between 390 and 2700 mg m^{-2} h^{-1}, with the maximum tidal mean fluxes occurring at day 188 and the lowest after day 192 (Fig. 7a). The average mass flux was 973 mg m^{-2} h^{-1} (SD 368 mg m^{-2} h^{-1}, $n = 131$). Although this trend was also visible in the mass flux of POC (Fig. 7b), it was much less clear due to the opposite trend in POC content as a percentage of total dry weight in the trap (Fig. 7c). The average POC content of all samples was 2.4% (SD 0.5%, $n = 131$) and the average CN ratio in the mass fluxes was 9.4 (SD 0.7, $n = 131$) with a maximum value of 11.5 at day 185 (Fig. 7d). Two exceptionally low ratios were measured in individual samples on day 189 (6.3) and day 194 (6.5), indicating a substantial contribution of fresh planktonic material on these days. In general the tidal mean CN ratio in the mass fluxes showed a slight decrease from about 10 in the first days to about 9 at the end of the measurements.

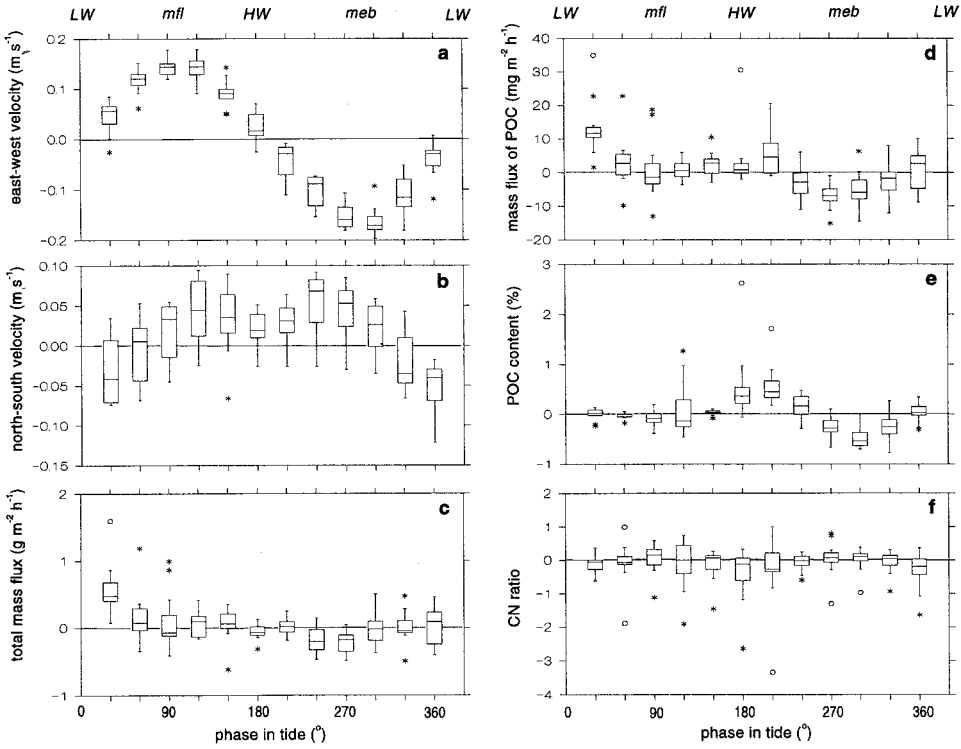

Figure 8. Box-whisker plots of the mean tidal cycle of (a,b) current velocity; (c) total mass flux of dry weight in the sediment trap; (d) mass flux of POC; (e) POC content of particles trapped; (f) atomic CN ratio of the organic matter trapped. All data are relative to the median values in Figure 7. Thus, negative values indicate that a parameter is below the tidally median, positive values that it is above.

The box-whisker plots in Figure 7 indirectly point to considerable variability within a single tidal cycle. To clarify this variability we divided the tidal cycle in 12 phase intervals of 30° each (corresponding to about 1 h) and positioned the 1 h interval trap data according to these phase intervals. Subsequently we subtracted the median mass flux (POC, CN ratio) of each tidal cycle from the 1 h interval values of that cycle. Thus we obtained 11 data points corresponding to 11 days of trap deployment in each of the 12 phase intervals, and corrected for the 14 days trend. For reference, similar plots were constructed for current velocity after selecting and integrating the corresponding intervals from the 'continuous' current velocity time series (Fig. 8a,b).

On average the total mass flux (dry weight, Fig. 8c) peaked in the first hour after LW and had its lowest value around maximum ebb current. On average the mass fluxes were higher during the flood current than during ebb. The flux of POC had peak values in the first hour after both slack tides (Fig. 8d) and, as for total mass flux, the total flux of POC was highest during flood current. During both flood and ebb tide minimum fluxes of POC occurred

around maximum current velocity. When expressed as a percentage of the total mass flux, the POC content of the trapped particles showed a slight decrease from LW to maximum flood current followed by a sharp increase to high contents during the 2 h around HW (Fig. 8e). After this peak the POC contents decreased to their lowest value at maximum ebb current velocity and subsequently increased again close to LW. The two extreme values in Figure 8e around HW correspond to the samples with relatively low CN ratios on days 189 and 194. On average the CN ratio showed only minor variations during the tidal cycle, although there was a slight tendency for lower ratios during HW and higher ratios during maximum current velocity (Fig. 8f).

f. Model results

The model outlined in Eq. (2) was tuned by comparing TSM calculated for 4.5 mab with the transmission data at the same depth (Fig. 9b). Initial values were 1 g m^{-3} for the column averaged TSM concentration $\langle C \rangle$ and 30 g m^{-2} for the mass of particles M_r in the fluff sediment layer. The parameter values are summarised in Table 2. The enhanced settling rate of 2.5×10^{-4} m s^{-1} after resuspension of particles from the fluff layer (Table 2) agrees with the range of values given by Jago *et al.* (1993) for their station B which was near our mooring site. With $\beta_r = 5 \times 10^{-5}$ s^{-1} and M_r typically between 10 and 100 g m^{-2} (Fig. 9c), the term $\beta_r \cdot M_r = 0.5 \times 10^{-3} - 5 \times 10^{-3}$ g m^{-2} s^{-1}, which is also within the range given by Jago *et al.* (1993).

Friction velocities exceeding the assumed threshold for resuspension of 8×10^{-3} m s^{-1} were not found before day 188, around maximum ebb current between days 188 and 192, around both maximum ebb and maximum flood current between days 192 and 196, and irregularly after day 196 (Fig. 9a). Thus the increase of TSM predicted by the model and observed in the data between days 186 and 188 (Fig. 9b) is caused by advection of particles with a low settling velocity and not by local resuspension. The first resuspension event on day 188 causes a peak in TSM at 0.2 mab followed by enhanced sedimentation. Together with the decreased tidally averaged advection of turbid waters from the south (Fig. 6d,e) this explains the low TSM concentrations on day 189. Although the model accurately predicts the resuspension peaks between days 189 and 192 the overall increase in TSM due to a combination of advection and resuspension lags behind the observational data in this period. A similar discrepancy is present after day 198. Between days 194 and 198 the model predicts the TSM concentrations reasonably well, including the strong decrease around day 197, which, similarly to day 189, seems to be caused by the absence of resuspension together with a lower net tidal advection of water from the south.

In line with the *in situ* data, the model simulated strong vertical gradients in TSM, particularly close to the sediment surface (Fig. 9c). Distinct peaks of friction velocity between days 188 and 192 and at day 196 are well reflected in corresponding peaks of TSM calculated for 0.2 mab. These resuspension maxima are, however, smoothed out considerably higher up in the water column. Also between days 192 and 196 when the friction velocity was above the threshold for resuspension most frequently, TSM above 6 mab

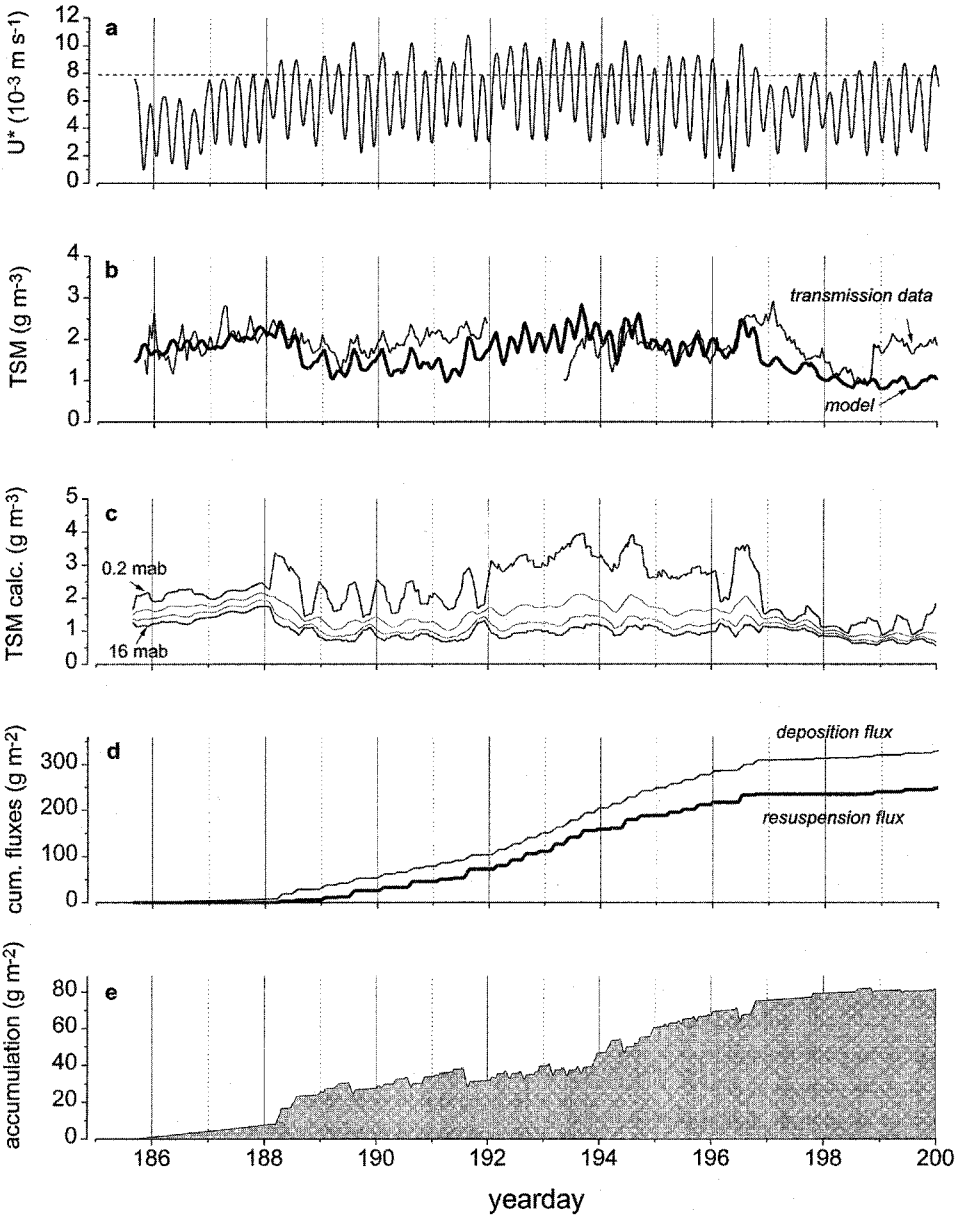

Figure 9. Results of the advection-deposition-resuspension model. (a) Friction velocity U^* calculated from current meter data. Note the spring-neap cycle with high velocities around days 192–194 and lower velocities on days 186 and 198. (b) TSM calculated at 4.5 mab (thick line, 3 h moving average) and estimated from transmission data at the same depth (thin line, 1 data point per hour). (c) TSM calculated at different depths in the lower water column (0.2, 6, 11 and 16 mab). (d) Calculated cumulative fluxes of deposition, resuspension and net accumulation (= deposition − resuspension) of particulate matter on the seafloor.

Table 2. Parameter values applied in the advection-deposition-resuspension model of TSM (Eqs. 1–6).[1,2] calculated from the spatial distribution of TSM at 6 mab (Fig. 3);[3] based on Tett and Walne (1995);[4] based on Jago *et al.* (1993), Pohlman and Puls (1995) and Tett and Walne (1995);[5,6,7] estimated by calibrating the model with the field data; Settling velocity 2 represents the increased average settling rate of TSM after a resuspension event.

Name	Symbol	Value	Unit
east-west gradient of TSM	$\partial C/\partial x$	1×10^{-4}	g m^{-4}[1]
north-south gradient of TSM	$\partial C/\partial y$	-1×10^{-4}	g m^{-4}[2]
threshold friction velocity	$U_{*,r}$	8×10^{-3}	m s^{-1}[3]
settling velocity 1	ω	2×10^{-5}	m s^{-1}[4]
settling velocity 2	ω	2.5×10^{-4}	m s^{-1}[5]
entrainment rate constant	β_r	5×10^{-5}	s^{-1} α[6]
background concentration	C_{back}	0.3	g m^{-3}[7]

remained relatively low indicating that resuspended particles stayed close to the bottom. Averaged over the entire period the deposition flux is slightly higher than the flux caused by resuspension (Fig. 9d). In total $\sim$75 g m^{-2} had cumulated on the seafloor, the bulk of the accumulation occurring on days 188 and 194–195.

4. Discussion

a. Sources of TSM

The mooring site in the Oyster Grounds is just north of the transition from the vertically well mixed southern North Sea, with high TSM concentrations, to the Central North Sea, which is stratified during summer and is less turbid (Eisma and Kalf, 1987). In the Oyster Grounds TSM mostly shows a gradient from south-east to north-west in the summer months, with concentrations between 0.5 and 2 mg l^{-1} below the thermocline (Fig. 3; Wirth and Seifert, 1988; Hölemann and Wirth, 1988; Dyer and Moffat, 1993). The highest turbidity is probably present $\sim$90 km southwest of the mooring in the vicinity of a tidal mixing front ('Frisian Front') where the water depth is slightly less, 30–40 m, than the Oyster Grounds proper (Van Haren and Joordens, 1990). Close to this front is a mud patch (Creutzberg *et al.,* 1984) from which particles may be resuspended and which may contribute to TSM at our mooring site. Contribution of other sources further away can, however, not be excluded. Moreover, the mud patch itself has been identified as an area where particles can be deposited (temporarily) that originate from the entire Southern Bight and the English coast (Creutzberg and Postma, 1979; Creutzberg *et al.,* 1984). Thus, the ultimate, longer-term sources of TSM observed at the mooring site are likely to be found in a large area south of the Oyster Grounds.

To determine whether the resuspended particles have the same properties as the top 2.5 mm of the sediment we follow the approach of Jago *et al.* (1993) and apply the two-component mixing model of Morris *et al.* (1987). In this model it is assumed that TSM consists of a constant background S_0 with carbon content C_0 and a variable amount of particles, S_r, resuspended from the sediment that have a carbon content C_r. Taking into

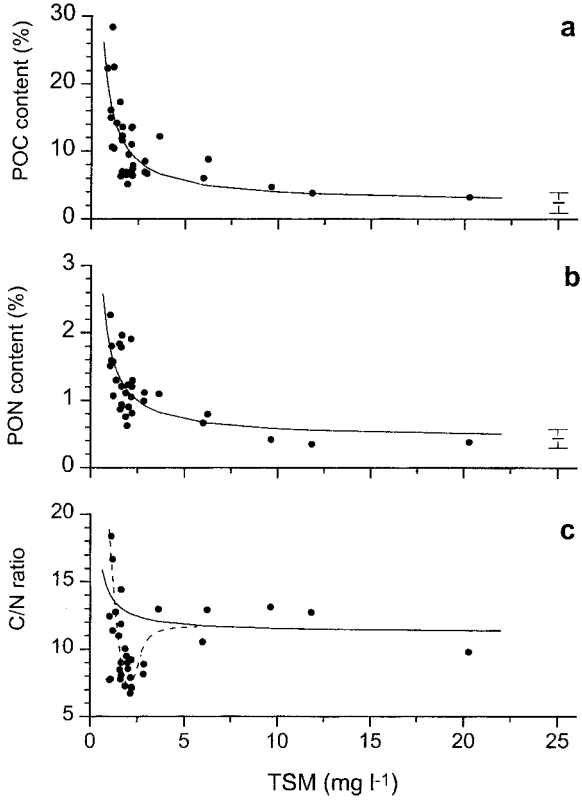

Figure 10. Relationships between (a) organic carbon content, (b) organic nitrogen content, and (c) CN ratio of TSM and the concentration of TSM in pump (0.2 mab) and bottle samples from the lower water column (6 and 11 mab). The regression line in A represents the relation POC = $15.2_{(SD=2.5)}/TSM + 2.4_{(SD=1.5)}$, $n = 36$, $R = 0.72$; in B: PON = $1.37_{(SD=0.25)}$/TSM + $0.44_{(SD=0.14)}$, $n = 36$, $R = 0.71$. Error bars in (a,b) indicate the POC, PON contents ± one standard deviation estimated for very large values of TSM. Lines in (c) are tentative and show the general trend (solid) and the dip in CN ratio around TSM = 2 mg l^{-1} (dashed).

account that TSM = $S_0 + S_r$ an inverse relationship follows between the organic carbon content of the mixture suspended in the water column (POC) and the total mass of that mixture (TSM):

$$\mathrm{POC} = (C_0 - C_r)\frac{S_0}{\mathrm{TSM}} + C_r. \tag{7}$$

Regression of POC against TSM in samples from the bottom mixed layer (0.2, 6, 11 mab) yields a significant relationship (Fig. 10a) from which C_r is calculated at 2.4% (SD = 1.5%). This carbon content is ~10 times higher than in the upper mm's of the sediment, ~5 times lower than on average in the water column, but equal to the average organic carbon content

in the sediment trap mass fluxes. If we do a similar analysis for organic N (Fig. 10b) it follows that the resuspension flux has an N content of 0.44% (SD = 0.14%) which again is close to the trap materials (0.30%). The organic carbon content in the resuspension flux found here confirms the data of Jago *et al.* (1993) who found C_r varying between 1.9% and 4.5% at two sites in the North Sea and in different months of the year. It is concluded that particles available for resuspension under non-storm conditions are carbon-enriched compared with the bulk sediment. This corroborates the view of Jago *et al.* (1993) and validates our modeling assumption that the materials resuspended are from a surficial fluff layer and not from the seabed proper. From the similarity of the C and N contents in the fluff material and in the sediment traps, it is further concluded that deposition of resuspended fluff materials is by far the dominating contributor to the trap mass fluxes.

Most of the labile carbon in the sediment originating from summer production is likely to be mineralized in winter or washed from the sediment (Van Raaphorst *et al.,* 1992). Thus, we estimated the 'base-line' POC content of the sediment on the basis of the 0.17% organic C measured by Van Raaphorst and Malschaert (1996) in the upper 5 mm of the sediment at the mooring site in February 1992. Using this value and POC = 0.24% and 2.4% in the bulk sediment and the fluff material, respectively, it follows that only ~3% of the sediment in the Oyster Grounds consists of fluff available for resuspension under the hydrodynamic conditions that prevailed during our study.

Not only POC in the resuspension flux can be estimated from the regression line in Figure 10a, but, if S_0 is known, also the C content in the suspended background (C_0). The steepness of the hyperbolic regression curve at low TSM values, however, makes the reliability of such estimate very sensitive to the accuracy of S_0. Using the background TSM concentration of 0.3 mg l^{-1} estimated from our modeling exercise (Table 2) C_0 is calculated at 53% which is a rather high percentage. If, instead, we assume a slightly higher background of 0.5 mg l^{-1} a more realistic POC content of 33% is found. Comparing this latter percentage with the average POC content of TSM (Table 1) and the 2.4% carbon content calculated for the resuspension component, it is concluded that, on average, resuspended fluff may contribute as much as about 70–80% to TSM in the bottom mixed layer.

b. Phytoplankton

A small part of TSM in the bottom mixed layer consisted of phytoplankton. At the average chlorophyll-*a* concentration of ~0.8 µg l^{-1} (Fig. 6f) and assuming an algal POC:chlorophyll-*a* ratio of 50–100:1 (Reid *et al.,* 1990) we estimate the average phytoplankton concentration at 0.04–0.08 mg-C l^{-1}, corresponding to 0.1–0.2 mg l^{-1} total biomass. Thus, the contribution of phytoplankton biomass to TSM is 10–20% in the lower part of the water column, but the contribution of phytoplankton C to total POC may be as large as 25–50%. Although these percentages are crude averages they demonstrate that living biomass and pigment containing detritus cannot be neglected as part of TSM, which,

consequently, not only consists of 'old' fluff materials but also, although for a minor part, of 'fresh' organic matter.

The relationships in Figure 10a,b obscure any further partition of TSM into old and fresh materials. Plotting the CN ratio of the suspended particles as a function of TSM, however, shows that at TSM = 1–3 mg l^{-1} the CN ratio is 6–10, which is less than at either lower or higher suspended matter concentrations (Fig. 10c). This indicates that labile, presumably plankton derived material dominates POC at low to moderate TSM concentrations, probably because phytoplankton production is stimulated in water masses with low TSM where light conditions are most favorable. Indeed, the highest chlorophyll-*a* concentrations were measured west of the mooring site where TSM was lowest and, in accordance, the tidal variability of chlorophyll-*a* is mainly due to east-west advective transport, which renders the semi-diurnal pattern with major peaks in fluorescence at HW. This is in contrast with TSM which is advected from the south-east and shows its peak values mainly during ebb current and LW, albeit additional maxima occurred around HW sometimes (e.g., Fig. 4).

Although the time series of TSM and chlorophyll-*a* are controlled by different processes and by advection from different directions, this does not mean that they behave completely differently without mutual influences. Close inspection of the time series in Figure (6f) reveals a quarter-diurnal pattern superimposed on the semi-diurnal pattern of chlorophyll-*a,* which is likely related to deposition of phytoplankton occurring at HW followed by resuspension at increasing current velocity (Jago *et al.,* 1993). Because some time passes between settling on the seafloor and re-entrainment in the water column, resuspended phytoplankton enters a new water mass enriched with TSM, thus providing conditions favorable for aggregation and floc-forming during the next LW. Flocculation may be further stimulated through binding of fluff particles with organic compounds derived from the phytoplankton (Eisma, 1992; Chen, 1995). This explains why sediment trap mass fluxes of phytopigments (Van Duyl *et al.,* 1997) and organic carbon (Fig. 8) are so high at LW despite the low phytoplankton concentrations in the water column in that phase of the tidal cycle.

c. Sediment trap fluxes

Even though wind and wave activity were low during the period of study, the C and N contents of the sediment trap mass fluxes indicated that these fluxes were primarily due to resuspension and resettling of bottom fluff, a situation which is characteristic for high-(tidal) energy environments (e.g., Gardner *et al.,* 1983). Thus, the trap fluxes cannot be used to directly determine the rate of mass accumulation on the sediment. Instead, they will be evaluated in order to elucidate tidal dynamics of both resuspension and resettling fluxes.

There is overwhelming evidence that the efficiency of sediment traps is controlled by their geometry, the mooring design and the hydrodynamic conditions during deployment (e.g., Gardner, 1985; Butman, 1986; Butman *et al.,* 1986; Baker *et al.,* 1988; Gust *et al.,* 1994). A general conclusion of these studies is that 'a sediment trap is a tool that cannot be

accurately calibrated at this time' (Gust *et al.,* 1994), and, consequently, that 'knowledge of the collection efficiency of sediment traps, particularly under conditions of varying current speed, is presently more a matter of hope than confidence' (Baker *et al.,* 1988). Despite this high level of uncertainty several recommendations have been made for optimal design and deployment that seem widely accepted.

We took these recommendations into account and applied a bottom-moored array containing a cylindrical trap with a relatively high aspect ratio (>4). As the current speed essentially varied between 2 and 20 cm s^{-1} the trap Reynolds number was between $4 \times 10^3 - 4 \times 10^4$. In this range of Reynolds numbers the collection efficiency of the trap is probably relatively insensitive to varying flow speeds (Butman, 1986), although a later study of Baker *et al.* (1988) revealed that lower efficiencies may be expected at the highest current velocities encountered during our study. The dimensionless fall velocity of the particles collected in the trap (ω/U = fall velocity/current velocity) cannot be quantified accurately from our data. Taking the range in tidal current speeds and assuming that the fall velocities estimated from the model (Table 2) are a good approximation for the real world, ω/U may vary over two orders of magnitude between 10^{-2} and 10^{-4}. There are both theoretical and experimental indications that the collection efficiency decreases with decreasing dimensionless fall velocity (e.g., Butman *et al.,* 1986; Baker *et al.,* 1988), thus suggesting that slowly settling particles may be under-collected at maximum current speeds in the tidal cycle. Gardner (1985), on the other hand, showed that smaller particles are collected more efficiently relative to larger ones when the trap is tilted in the direction of the current, which was always the case during our deployments.

Tilted traps collect more particles than traps held vertical (Gardner, 1985). It can, however, not be concluded whether, at a given current speed and trap Reynolds number, tilted traps are over-collectors or vertical traps are under-collectors. To investigate the possible effect of tilt on our trap mass fluxes we applied the tilt-correction determined for baffled cylinders with aspect ratio 5.2 by Gardner (1985):

$$F = \frac{F_T}{1 + 1.4 \sin 2\theta} \tag{8}$$

where F is the corrected mass flux expected in a vertical trap, F_T is the flux measured in the tilted trap and θ is the degree of tilt from the vertical. Correction for tilt yields considerably lower estimates of the settling mass fluxes, but the overall picture with highest fluxes in the first week of our measurements remains intact (Fig. 11a). For the mean tidal cycle, correction of the mass fluxes had a relatively minor effect (Fig. 11b) giving support to the conclusion that particularly the high mass fluxes shortly after LW are realistic.

Enhanced tidal mean total mass fluxes were measured between days 188 and 190 when also the highest fluxes were collected in individual sample cups (Fig. 7a, 11a). These high fluxes may also be inferred from the model, which simulated massive deposition on day 188 (Fig. 9d). Although TSM increased in the first week, this increase seems not sufficient to explain the high trap fluxes, certainly not when taking into account that TSM between

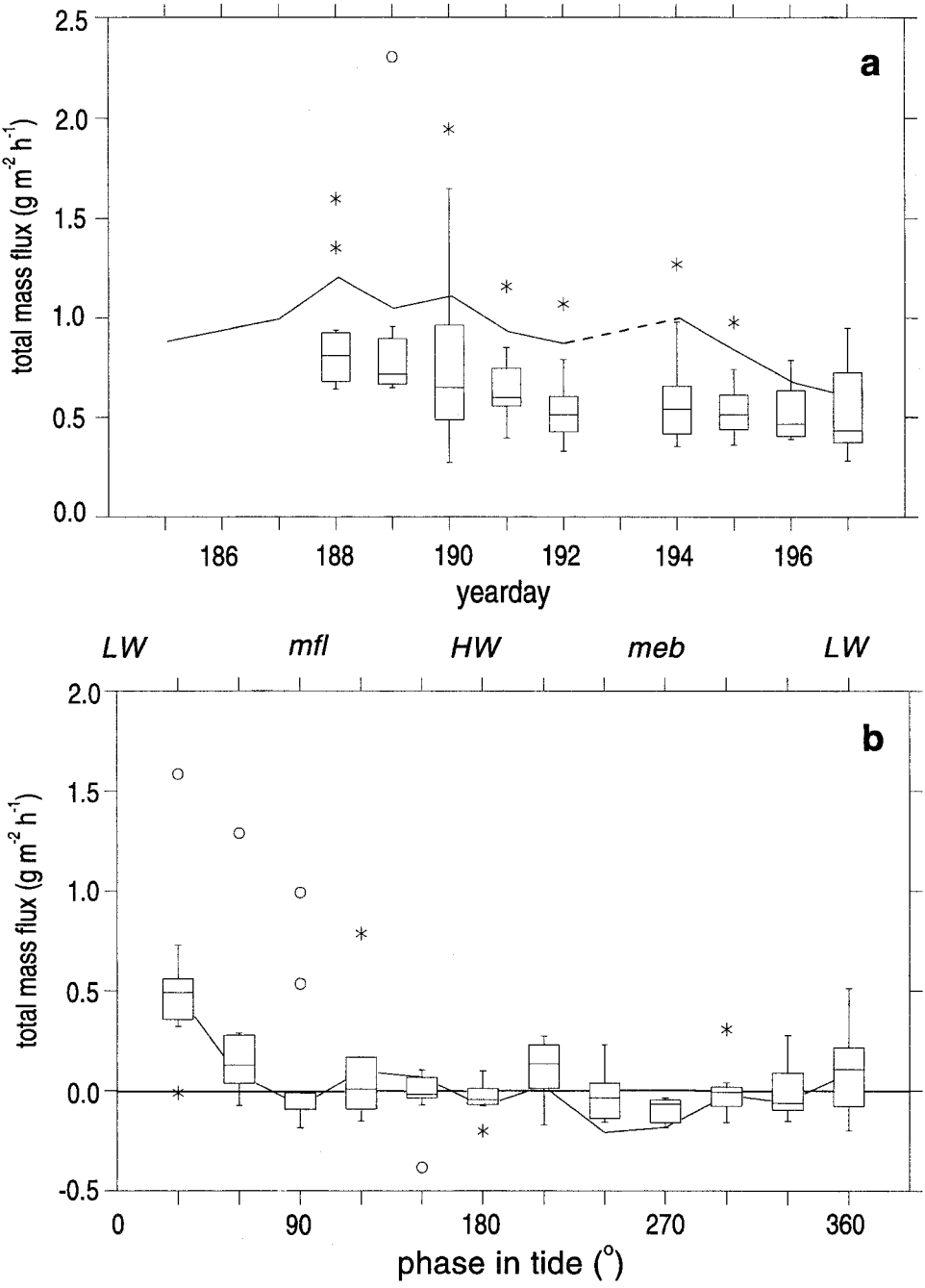

Figure 11. Total mass fluxes in the sediment trap corrected for tilt (box-whiskers) and median fluxes not corrected for tilt (solid line) obtained from Figure 7 and 8. (a) tidally averaged fluxes; (b) mean tidal cycle of the fluxes corrected for the 14 days trend.

day 191 and 197 was equally high as on day 188 and even higher than on day 189. Thus, it seems that the average settling velocity had increased from day 188 to 190. This is made clear by calculating the ratio between the mass fluxes and the TSM concentration, which can be viewed as the apparent settling velocity of the particles collected in the trap (Fig. 12). Assuming that the tilt-corrected fluxes are most close to reality, the apparent tidal mean settling velocity was about 1×10^{-4} m s^{-1} which is in between the low and high settling velocities estimated from our model. Higher median values of about 1.5×10^{-4} m s^{-1} were calculated for days 188 and 189 while velocities between 2.5×10^{-4} and 5×10^{-4} m s^{-1} occurred during four trap opening hours between days 188 and 190 at the onset of spring tide-related periods with enhanced bottom friction velocities. The same calculation shows a minimum tidal mean settling velocity on day 196 just before neap-tide.

Any further statement on the effect of the spring-neap cycle on the trap fluxes has to remain speculative because we sampled only one such cycle. The trap data span, however, a total of 11 semi-diurnal cycles and for these more definite conclusions can be drawn. On average the total mass flux was strongly elevated in the first hour after LW and lowest during maximum ebb current. The similarity of this pattern with that of the apparent settling velocity (Fig. 12b) demonstrates the importance of changes in particle settling velocity during the tidal cycle. Around maximum ebb current particles are resuspended from the seafloor and maximally advected from the south-east. At the relatively high current speed during that phase of the tidal cycle flocs are not likely to be formed and may even be broken up (e.g. Chen, 1995). The organic carbon content of the mass fluxes is relatively low at maximum ebb current indicating a poor association with detritus and phytoplankton derived compounds. This association increases upon approaching LW, as indicated by the re-increasing POC content after its minimum at maximum ebb current and the decreasing CN ratio, consistent with the conclusion made earlier that the high mass fluxes shortly after LW are caused by flocculation processes. Flocculation effects on the apparent settling velocity are more pronounced at LW than at HW. We conclude that floc formation is stimulated most efficiently at times of low current speeds directly after maximum concentrations of both chlorophyll-*a* and TSM have been advected past the mooring site, thus providing sufficient possibility for particle collision and aggregation.

d. Sediment

Resuspension, advection and redeposition alter the properties of the surface layers of the sediment. During periods of resuspension, sediment stratification and laminations may disappear, particularly close to the sediment surface (Aller, 1989). We observed a fluffy layer on top of the sediment in our box-core only during the first days of the cruise, i.e. during neap tide when the current velocity remained low. The disappearance of this layer coincides with the first day that the bottom friction velocity exceeded the threshold for resuspension assumed in the model. Other sediment properties like water content and organic carbon content in the top 5 mm, reached their highest values at the moment of massive deposition on day 188 shortly after the first resuspension event (Fig. 2, 9) when

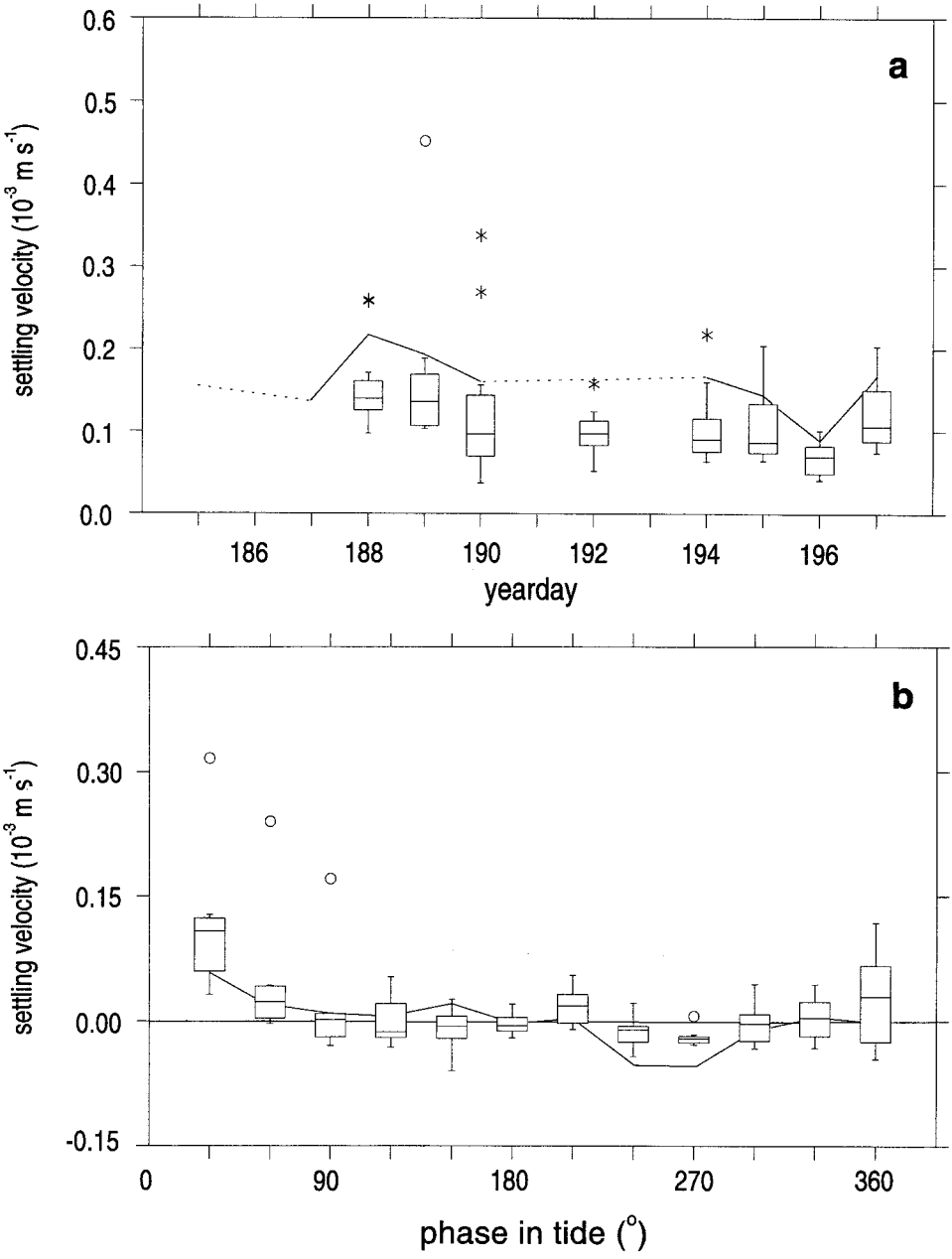

Figure 12. Apparent settling velocity (ω) of the particles collected with the sediment trap calculated as the ratio between the total mass flux in the trap and the TSM concentration measured at 4.5 mab with the transmissometer. Box-whiskers indicate values of ω that are based on mass fluxes corrected for tilt, the solid line the median values calculated using the uncorrected mass fluxes. a: tidally mean velocity; b: mean tidal cycle corrected for the 14 days trend.

also the trap fluxes were at maximum (Fig. 7), and decreased continuously in the period thereafter (Fig. 2). We interpret these observations as evidence for resuspension starting at day 188 at the onset of spring tide following steady deposition around neap tide.

The decrease in the water and organic carbon contents of the sediment at the beginning of spring tide suggests that fluff is washed out from the sediment. This contradicts model results and trap data showing that resuspended fluff resettled during slack current following resuspension. Apparently, this intermittent deposition did not lead to a watery fluff layer recognizable in the box-cores. An important mechanism by which fluffy layers are created is by feeding, locomotion and habitat development of the benthic fauna that, amongst other effects, leads to rhythmic fluff expulsions related to faeces production and caving (Davis, 1993). It may be that the benthic fauna changed its behavior during the spring-neap cycle. Suspension feeders probably diminish their activity at the high current speed at spring tide, thus having to take all their food at the subsequent slack current, while they may show an approximately constant activity around neap tide (Davoult and Gounin, 1995). In addition, some species may change from bed destabilizing (Davis, 1993) deposit feeding at low current speeds to passive suspension feeding at higher speeds (Thomsen *et al.,* 1995 and references cited therein). This may have promoted an efficient burial of resettled material during spring tide. According to Davis (1993) both the bed stabilizing and destabilizing effects caused by different species of benthic fauna increase with increasing seabed shear stress. The disappearance of the fluff layer from the top of the sediment then may simply reflect the high turn-over rate of resuspendable particles due to the increased gross fluxes of both resuspension and deposition during spring-tide.

e. Advection, resuspension and deposition in the Oyster Grounds

There are no good estimates available of the net transport time of TSM through the southern North Sea. The residence time of water estimated to be less than one year may serve as a minimum estimate only because temporary deposition and retention on the sea-floor should lengthen the average travelling time of particulate matter. It has been suggested (Kempe *et al.,* 1988) that the fine fraction of the sediment requires 10–15 years for the journey from the Elbe Estuary in the German Bight to the Skagerrak. Such a long travel time would guarantee almost complete oxidation of the labile organic matter before final deposition in the Skagerrak-Norwegian Channel. Thus, an important question to be answered is to what extent deposition and resuspension in the Oyster Grounds and similar areas influence the overall lateral transport of TSM and the fate of organic matter. We will first address the retention time of deposited particles in the sediment before their next resuspension under calm weather conditions, then discuss the possible influence of storms, and finally the role of mid-shelf depocenters in the carbon budget of the North Sea.

i. Residence times of particulate matter. A first estimate of the time scale for settling can be obtained from the model result on the gross deposition flux Q_b (Eq. 5) yielding a total of 325 g m^{-2} in 14 days (Fig. 9), which corresponds to an average flux of 23 g m^{-2} d^{-1}. At a

mean concentration of 1.5–2 g l^{-1} the inventory of TSM in the lower mixed layer of the water column is 30–40 g m^{-2}, from which a settling time of about 1.5 day is calculated. If, alternatively, the apparent sinking velocities calculated from the sediment trap data are used and if we assume an average settling distance of 10 m (half the thickness of the bottom mixed layer), the time needed for settling is estimated at about 10^5 s = 1.2 days. It is concluded that the residence time of particulate matter in the bottom mixed layer is of the order of 1–2 days.

The residence time in the water column should be compared to the time particles are retained in the sediment following deposition. According to our model, about 25% of the gross deposition flux is accumulated and, consequently, retained in the sediment until, at least, the first storm event that will cause net erosion. The other 75% of the particles deposited on the sediment is retained temporarily in the pool of accumulated fluff. From this pool, some particles are entrained in the water column whenever the bed friction velocity exceeds the threshold for resuspension. The average time these particles stay in the sediment can be estimated from the total pool of accumulated fluff, which is assumed to be available for entrainment, divided by the gross resuspension flux.

The model simulates a net accumulation of $\sim$75 g m^{-2} in the 14-day study period, suggesting that, at prolonged deposition for a period of weeks, the total inventory on the bottom can be several hundred grams per square meter. Obviously, this amount directly depends on the time the accumulation process remains undisturbed by storm events and also, the net accumulation calculated by the model is subject to some uncertainty. From the organic carbon content in the sediment and the resuspended fluff we have calculated earlier that about 3% of the mass present in the upper 5 mm of the sediment is available for resuspension. With this percentage and taking into account the volume occupied by pores (45%, as calculated from the water content) and assuming further a specific density of the sediment grains of 2.5 g cm^{-3}, we calculate that approximately 250 g m^{-2} of resuspendable fluff is present in the surface 5 mm of the sediment. Although this value directly depends on the depth of the sediment layer assumed to be involved in resuspension, the order of magnitude is equal to the amount calculated from our model and favors also with the accumulation calculated by Sündermann (1993) with his more elaborate model. The gross resuspension rate is taken from the model and amounts to 250 g m^{-2} in 14 days (Fig. 9). Taking a range of 100–250 g m^{-2} as a best guess for the pool of resuspendable fluff in the sediment, this means that the average residence time of particles between deposition and resuspension is of the order of 1–2 weeks under the calm weather conditions that prevailed during our study.

ii. Influence of storms. The accumulation of $\sim$75 g m^{-2} per 14 days would, if valid outside the study period, lead to a sediment accretion of approximately 1.5 mm per year. Previous studies have indicated that net accumulation is not likely to occur in the Oyster Grounds on time scales ranging from decades to centuries (Cadée, 1984; Eisma and Kalf, 1987). The summer deposition predicted by the laboratory experiments of Creutzberg and Postma

(1979) and the models of Puls and Sündermann (1990) and Sündermann (1993) is, however, confirmed by our study. Here, we will question whether such deposition can lead to accumulation even during stormy periods in autumn and winter. Therefore, we conducted additional simulations with our model, inserting current velocities measured at the mooring site in December 1994. Thus, we created 'storms' between days 190 and 195 with bottom friction velocities well above 10–15 $\times$ 10^{-3} m s^{-1} (Fig. 13). For comparability we left all parameters unchanged, except for the depth of the bottom mixed layer that we assumed now to occupy the whole water column of 46 m (i.e. no stratification). Neither did we take the effect of waves into account, which means that the results can be interpreted in a qualitative sense only. Despite the absence of wave effects the model reproduced the development of TSM concentration as revealed by the backscatter intensity from an acoustic Doppler current profiler (ADCP) reasonably well, particularly the timing of the strong peaks in TSM associated with maximum friction velocities (Fig. 13).

The picture that emerges from the model is a highly dynamic exchange of particles between the sediment and the water column at increased friction velocities. Compared to the calm-weather simulation (Fig. 9) the gross fluxes of both resuspension and deposition were much higher in the stormy winter situation and almost complete erosion of the bottom fluff layer occurred at the highest friction velocities. The resuspension fluxes are probably even underestimated due to the absence of the effect of wave action in our calculations. Therefore, we may expect that in stormy (winter) conditions large amounts of the materials deposited during previous calm (summer) periods are eroded. Both the data from the ADCP and the model results show, however, that rapid resettling occurs after passage of the storms, albeit that concentrations after the storms remained slightly higher than before.

iii. The role of temporary depocenters in North Sea carbon cycling. Basically, temporary depocenters function as an area to which TSM is advected and in which this particulate matter is retained for some time in the sediment following deposition. Upon resuspension the particles are advected from the area and re-enter the main cross-shelf transport route. During their retention in the sediment, particles are reworked and can lose a substantial portion of their organic C content. Thus, TSM entering an area as the Oyster Grounds are, on average, probably of better quality and contain more labile organic C than the particles leaving the area.

Thomsen *et al.* (1995) reported results from an *in situ* experiment on a several kilometers long transect occupied by macrofauna feeding at the sediment-water interface along the continental slope of the Barents Sea, and showed that laterally advected POC was the most important source of labile carbon to the benthic community. In the Oyster Grounds, a similar importance of advection of organic matter may exist. In the absence of sufficient deposition from local primary production in the water column, TSM and POC advected to the Oyster Grounds may sustain deposition fluxes and provide organic matter to the benthos. The calculated net deposition of 75 g m^{-2} corresponds to a daily input of organic carbon of about 115 mg m^{-2} to the sediment (assuming a labile carbon content of

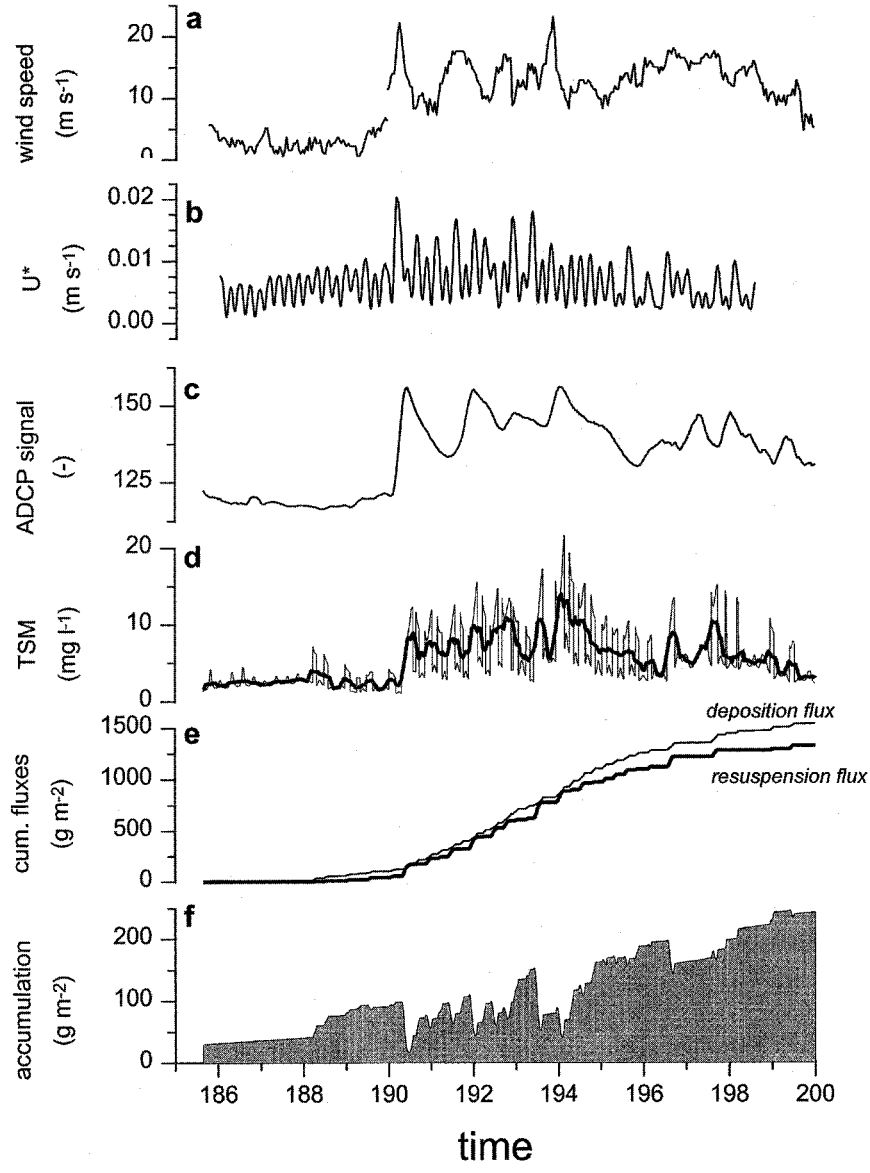

Figure 13. Results of a model simulation with storms. Wind and current speeds measured in December 1994 were inserted in the original data set (Fig. 6) starting on day 190. (a) wind speed at 10 m above the water surface; (b) bottom friction velocity U^* as calculated from the current meter data; (c) ADCP backscatter signal (relative units) indicating TSM concentrations at 4 mab; (d) calculated TSM concentrations at 4.5 mab; (e) calculated cumulative gross fluxes of resuspension and deposition; (f) calculated net accumulation on the sediment.

2.4–0.2 = 2.2%), which is sufficient to fuel the local benthic bacterial production (32 mgC m^{-2} d^{-1} in the top 3 mm, Van Duyl *et al.* 1997). This comparison is biased as it assumes complete availability for the bacterial population of the organic matter accumulated within the time-scale considered and because it ignores the carbon utilization by meiofauna and macrofauna. It does not, however, take into account the amount of organic matter that is not accumulated but which is deposited temporarily and, during its stay in the sediment, is available as carbon source for the benthic organisms.

According to the measurements of Van Duyl *et al.* (1997) sediment concentrations of the phytopigments chlorophyll-*a*, fucoxantine and pheophytin-*a* decreased at a first order rate of ~0.06 d^{-1} between days 185 and 199, corresponding to a turn-over time of 17 days. This turn-over is determined by a balance of decomposition, new input of phytopigments and dilution by the deposition of particles relatively poor in phytopigments. Consequently, the average life-time of phytopigments in the sediment may differ somewhat from the turn-over time calculated from the above rate of disappearance. Furthermore, the degradation of pigments may be more rapid than other sedimentary organic compounds that may serve as food for the benthos (Van Duyl *et al.,* 1997). The decomposition rate for fresh phytoplankton debris of about 10 y^{-1} mentioned in the introduction corresponds to a turn-over time of about 5 weeks. It is concluded that a considerable portion of the organic matter deposited is mineralized in a few weeks only, i.e. at time scales comparable to the average retention of fluff particles in the sediment between deposition and resuspension.

A rapid mineralization of organic matter shortly after deposition is in accordance with sediment-water exchange fluxes and pore water profiles of inorganic nutrients at this station and in comparable areas with transient deposition in the North Sea (Gehlen *et al.,* 1995; Lohse *et al.,* 1995; Van Raaphorst and Malschaert, 1996). Such rapid microbial decomposition is probably promoted by frequent resuspension and physical stirring of the sediment (Aller, 1989). Furthermore, the rich macrofauna assemblage at the site may provide an additional stimulus for particle reworking and organic breakdown. We conclude that substantial decomposition can occur of the organic matter settled in the Oyster Grounds before re-entrainment into the cross-shelf transport route towards the Skagerrak-Norwegian Channel. Taking into account that repeated deposition and resuspension may occur on this route, this conclusion implies that mid-shelf temporary depocenters play a crucial role in the carbon budget of the North Sea.

Acknowledgments. We are grateful to Willem Polman and the crew of RV *Pelagia* for their help during the cruise. Lutz Lohse did part of the sediment sampling on board. Fleur van Duyl and Herman Ridderinkhof critically read early drafts of the manuscript. This study was funded by the Dutch BEON Programme (grant 94/95 E-01) and by the Netherlands Marine Research Foundation (NWO-GOA grant 39104). HVH has been supported by a grant from the Dutch Organization for the Advancement of Scientific Research (NWO). This is NIOZ contribution no. 3108.

REFERENCES

Aller, J. Y. 1989. Quantifying sediment disturbance by bottom currents and its effect on benthic communities in a deep-sea western boundary zone. Deep-Sea Res., *36,* 901–934.

Baker, E. T., H. B. Milburn and D. A. Tennant. 1988. Field assessment of sediment traps under varying flow conditions. J. Mar. Res., *46,* 573–592.

Butman, C. A. 1986. Sediment trap biases in turbulent flows: Results from a laboratory flume study. J. Mar. Res., *44,* 645–693.

Butman, C. A., W. D. Grant and K. D. Stolzenbach. 1986. Predictions of sediment trap biases in turbulent flows: A theoretical analysis based on observations from the literature. J. Mar. Res., *44,* 601–644.

Cadée, G. C. 1984. Macrobenthos and macrobenthic remains on the Oyster Ground, central North Sea. Neth. J. Sea Res., *18,* 160–178.

Chen, S. 1995. Floc size and aspects of flocculation processes of suspended particulate matter in the North Sea area. Ph.D. thesis, University of Utrecht, Netherlands.

Churchill, J. H., P. E. Biscaye and F. Aikman III. 1988. The character and motion of suspended particulate matter over the shelf edge and upper slope off Cape Cod. Cont. Shelf Res., *8,* 789–809.

Churchill, J. H., C. D. Wirick, C. N. Flagg and L. J. Pietrafesa. 1994. Sediment resuspension over the continental shelf east of the Delmarva Peninsula. Deep-Sea Res., II, *41,* 341–363.

Creutzberg, F. and H. Postma. 1979. An experimental approach to the distribution of mud in the southern North Sea. Neth. J. Sea Res., *13,* 99–116.

Creutzberg, F., P. Wapenaar, G. Duineveld and N. Lopez Lopez. 1984. Distribution and density of the benthic fauna in the southern North Sea in relation to bottom characteristics and hydrographic conditions. Rapp. P.-v. Réun. Conts. Int. Explor. Mer., *183,* 101–110.

Davis, W. R. 1993. The role of bioturbation in sediment resuspension and its interaction with physical shearing. J. Exp. Mar. Biol. Ecol., *171,* 187–200.

Davoult, D. and F. Gounin. 1995. Suspension-feeding activity of a dense *Ophiuthrix fragilis* (Abildgaard) population at the water-sediment interface: time coupling of food availability and feeding behaviour of the species. Estuar. Coast. Shelf Sci., *41,* 567–577.

Drake, D. E. and D. A. Cacchione. 1989. Estimates of the suspended sediment reference concentration and resuspension coefficient (γ_0) from near-bottom observations on the California shelf. Cont. Shelf Res., *9,* 51–64.

Dyer, K. R. and T. J. Moffat. 1993. Suspended sediment distributions in the North Sea. Inst. Marine Studies Report, Univ. of Plymouth.

Eisma, D. 1992. Suspended Matter in the Aquatic Environment. Springer, Berlin.

Eisma, D. and J. Kalf. 1987. Dispersal, concentration and deposition of suspended matter in the North Sea. J. Geol. Soc., *144,* 161–178.

Gardner, W. D. 1985. The effect of tilt on sediment trap efficiency. Deep-Sea Res., *32,* 349–361.

Gardner, W. D., M. J. Richardson, K. R. Hinga and P. E. Biscaye. 1983. Resuspension measured with sediment traps in a high-energy environment. Earth Planet. Sci. Lett., *66,* 262–278.

Gehlen, M., J. F. P. Malschaert and W. Van Raaphorst. 1995. Spatial and temporal variability of benthic silica fluxes in the southeastern North Sea. Cont. Shelf Res., *15,* 1675–1696.

Gust, G., A. F. Michaels, R. Johnson, W. G. Deuser and W. Bowles. 1994. Mooring line motions and sediment trap hydromechanics: *in situ* intercomparison of three common deployment designs. Deep-Sea Res., *41,* 831–857.

Hainbucher, D., T. Pohlman and J. Backhaus. 1987. Transport of conservative passive tracers in the North Sea: first results of a circulation and transport model. Cont. Shelf Res., *7,* 1161–1179.

Hill, P. S. and A. R. M. Nowell. 1995. Comparison of two models of aggregation in continental-shelf bottom boundary layers. J. Geophys. Res., *100,* 22,749–22,763.

Hölemann, J. and H. Wirth. 1988. Concentration, major element ratios and scanning electron microscopy of suspended particulate matter from the North Sea, spring 1986. Mitt. Geol.-Paläont. Inst. Univ. Hamburg, SCOPE/UNEP, Sonderband *65,* 183–206.

Jago, C. F., A. J. Bale, M. O. Green, M. J. Howarth, S. E. Jones, I. N. McCave, G. E. Millward, A. W. Morris, A. A. Rowden and J. J. Williams. 1993. Resuspension processes and seston dynamics, southern North Sea. Phil. Trans. R. Soc. Lond., *A343,* 475–491.

Jenness, M. I. and G. C. A. Duineveld. 1985. Effects of tidal currents on chlorophyll-*a* content of sandy sediments in the southern North Sea. Mar. Ecol. Prog. Ser., *21,* 283–287.

Jørgensen, B. B. 1983. Processes at the sediment-water interface, *in* The Major Biogeochemical Cycles and Their Interactions, B. Bolin and R. B. Cook, eds., Wiley, Chichester, 477–515.

Kempe, S. and T. Jennerjahn. 1988. The vertical particle flux in the northern North Sea, its seasonality and composition. Mitt. Geol.-Paläont. Inst. Univ. Hamburg, SCOPE/UNEP, Sonderband, *65,* 229–268.

Kempe, S., G. Liebezeit, V. Dethlefsen and U. Harms. 1988. Biogeochemistry and distribution of suspended matter in the North Sea and implications to fisheries biology. Synopsis. Mitt. Geol.-Paläont. Inst. Univ. Hamburg, SCOPE/UNEP, Sonderband *65,* XI–XXIV.

Krone, R. B. 1962. Flume studies of the transport of sediment in estuarial shoaling processes. Hydr. Engr. Lab. and Sanitary Engr. Res., Lab., Univ. of California, Berkeley, 110 pp.

Lohse, L., J. F. P. Malschaert, C. P. Slomp, W. Helder and W. Van Raaphorst. 1995. Sediment-water fluxes of inorganic nitrogen compounds along the transport route of organic matter in the North Sea. Ophelia, *41,* 173–197.

Lyne, V. D., B. Butman and W. D. Grant. 1990a. Sediment movement along the U.S. east coast continental shelf-I. Estimates of bottom stress using the Grant-Madsen model and near-bottom wave and current measurements. Cont. Shelf Res., *10,* 429–460.

—— 1990b. Sediment movement along the U.S. east coast continental shelf-II. Modelling suspended sediment concentration and transport rate during storms. Cont. Shelf Res., *10,* 397–428.

McCave, I. 1987. Fine sediment sources and sinks around the East Anglian coast (UK). J. Geol. Soc. Lond., *144,* 149–152.

Middelburg, J. J. 1989. A simple rate model for organic matter decomposition in marine sediments. Geochim. Cosmochim. Acta, *53,* 1577–1581.

Moody, J. A., B. A. Butman and M. H. Bothner. 1987. Near-bottom suspended matter on the continental shelf during storms: estimates based on *in situ* observations of light transmission and a particle size dependent transmissometer calibration. Cont. Shelf Res., *7,* 609–628.

Morris, A. W., A. J. Bale, R. J. M. Howland, R. F. C. Mantoura and E. M. S. Woodward. 1987. Controls of the chemical composition of particle populations in a macrotidal estuary (Tamar estuary, UK). Cont. Shelf Res., *7,* 1351–1355.

Nedwell, D. B., R. J. Parkes, A. C. Upton and D. J. Assinder. 1993. Seasonal fluxes across the sediment-water interface, and processes within sediments. Phil. Trans. R. Soc. Lond., *A343,* 519–529.

Otto, L., J. T. F. Zimmerman, G. K. Furness, M. Mork, R. Saetre and G. Becker. 1990. Review of the physical oceanography of the North Sea. Neth. J. Sea Res., *26,* 161–238.

Pingree, R. D. and D. K. Griffiths. 1978. Tidal fronts on the shelf seas around the British Isles. J. Geophys. Res., *83,* 4615–4622.

Pohlman, T. and W. Puls. 1995. Currents and transport in water, *in* Circulation and Contamination Fluxes in the North Sea, J. Sündermann, ed., Springer, Berlin, 345–402.

Postma, H. and J. W. Rommets. 1984. Variations of particulate organic carbon in the central North Sea. Neth. J. Sea Res., *18,* 31–50.

Puls, W. and J. Sündermann. 1990. Simulation of Suspended Sediment Dispersion in the North Sea, *in* Residual Currents and Long-Term Transport, Coastal and Estuarine Studies, *38,* R. T. Cheng ed. Springer New York, 356–372.

—— 1993. Modeling the distribution of suspended matter and lead in the North Sea, *in* Nearshore and Estuarine Cohesive Sediment Transport, Coastal and Estuarine Studies, *42,* A. J. Mehta, ed., Springer New York, 520–540.

Reid, C. P., C. Lancelot, W. W. C. Gieskes, E. Hagmeier and G. Weichart. 1990. Phytoplankton of the North Sea and its dynamics: A review. Neth. J. Sea. Res., *26,* 295–331.

Ruardij, P., H. Van Haren and H. Ridderinkhof. 1997. The impact of timing of the thermal stratification on production, succession and grazing of phytoplankton in shelf seas: A model study. J. Sea. Res., in press.

Sündermann, J. 1993. Suspended particulate matter in the North Sea: field observations and modelling. Phil. Trans. R. Soc. Lond., *A343,* 45–52.

Tett, P. and A. Walne. 1995. Observations and simulations of hydrography, nutrients and plankton in the southern North Sea. Ophelia, *42,* 371–416.

Thomsen, L., G. Graf, K. von Juterzenka and U. Witte. 1995. An *in situ* experiment to investigate the depletion of seston above an interface feeder field on the continental slope of the western Barents Sea. Mar. Ecol. Prog. Ser., *123,* 295–300.

Tijssen, S. B. and F. J. Wetsteyn. 1984. Hydrographic observations near a subsurface drifter in the Oyster Ground, North Sea. Neth. J. Sea Res., *18,* 1–12.

Van Duyl, F. C., G. C. A. Duineveld, A. J. Kop and G. Kraay. 1997. Pelagic-benthic coupling in the North Sea: short-term dynamics in phytopigment sedimentation and the response of benthic bacteria. Aquat. Micron. Ecol., *13,* 47–61.

Van Haren, J. J. M. and J. C. A. Joordens. 1990. Observations of physical and biological parameters at the transition between the southern and the northern North Sea. Neth. J. Sea Res., *25,* 331–350.

Van Raaphorst, W., H. T. Kloosterhuis, E. M. Berghuis, A. J. Gieles, J. F. P. Malschaert and G. J. van Noort. 1992. Nitrogen cycling in two types of sediments of the southern North Sea (Frisian Front, Broad Fourteens): Field data and mesocosm results. Neth. J. Sea Res., *28,* 293–316.

Van Raaphorst, W. and J. J. F. Malschaert. 1996. Ammonium adsorption in superficial North Sea sediments. Cont. Shelf Res., *16,* 1415–1435.

Van Weering, T. C. E., G. W. Berger and J. Kalf. 1987. Recent sediment accumulation in the Skagerrak, north eastern North Sea. Neth. J. Sea Res., *21,* 177–189.

Verardo, D. J., P. N. Froelich and A. McIntyre. 1990. Determination of organic carbon and nitrogen in sediments using the Carlo Erba NA-1500 analyzer. Deep-Sea Res., *37,* 157–165.

Walsh, I. J., J. Dymond and R. Collier. 1988. Rates of recycling of biogenic components of settling particles in the ocean derived from sediment trap experiments. Deep-Sea Res., *35,* 43–58.

Walsh, J. J. 1991. Importance of continental margins in the marine biogeochemical cycling of carbon and nitrogen. Nature, *350,* 53–55.

Wirth, H. and R. Seifert. 1988. Mineralogy, geochemistry and SEM-observations of suspended particulate matter from the North Sea, spring 1984. Mitt. Geol.-Paläont. Inst. Univ. Hamburg, SCOPE/UNEP, Sonderband *65,* 163–181.

Wright, L. D. 1995. Morphodynamics of inner continental shelves. CRC Marine Science Series, CRC Press, Boca Raton, Florida, USA, 241.

Received: *12 December, 1996;* revised: *15 July, 1997.*